Interplay of Collective and Single Particle Modes in the Continuum: Structure and Reactions

F. Barranco

Sevilla University

R.A. Broglia

Milano University and INFN; NBI, Copenhagen

G. Colo', A. Idini, E. Vigezzi

Milano University and INFN

K. Mizuyama

Osaka University

G. Potel

CEA, Saclay

Outline

- A model for one- (^{11}Be, ^{10}Li, ^{9}He..) and two-neutron halo nuclei (^{12}Be, ^{11}Li, ^{10}He…) including core polarization effects

- Test of the model: two-nucleon transfer reactions

- Calculation of single-particle self-energy in coordinate space with effective forces; optical potentials

- Renormalization of the pairing field in neutron stars

Overview

A key challenge for *ab-initio* theory is to describe and predict properties of medium mass nuclei from the valley of stability towards the driplines, especially in relation to the wealth of new experimental data now coming from radioactive beam facilities. The nuclear many-body problem is a difficult undertaking from both the computational and theoretical points of view. Techniques such as Green's function Monte Carlo (GFMC) and no-core shell model (NCSM) allow essentially exact calculations, but are limited to light nuclei. For mid-mass isotopes above A=16, the challenge posed by the numerical scaling demands innovative many-body theory techniques and computational approaches. This is especially true for the extensions to nuclei with an open-shell character. Techniques such as self-

	E (MeV)			
	CDB2k	INOY		Exp.
^{6}Li	29.07(41)	32.33(19)	[32.07]	31.99
^{7}Li	35.56(23)	39.62(40)	[38.89]	39.24
^{8}Li	35.82(22)	41.27(51)	[39.94]	41.28
^{9}Li	37.88(82)	45.86(74)	[42.30]	45.34
^{11}Li	37.72(45)	42.50(95)[a]	[40.44]	45.72(1)

[a]The exponential convergence rate is not fully reached.

Still a challenge: ^{11}Li

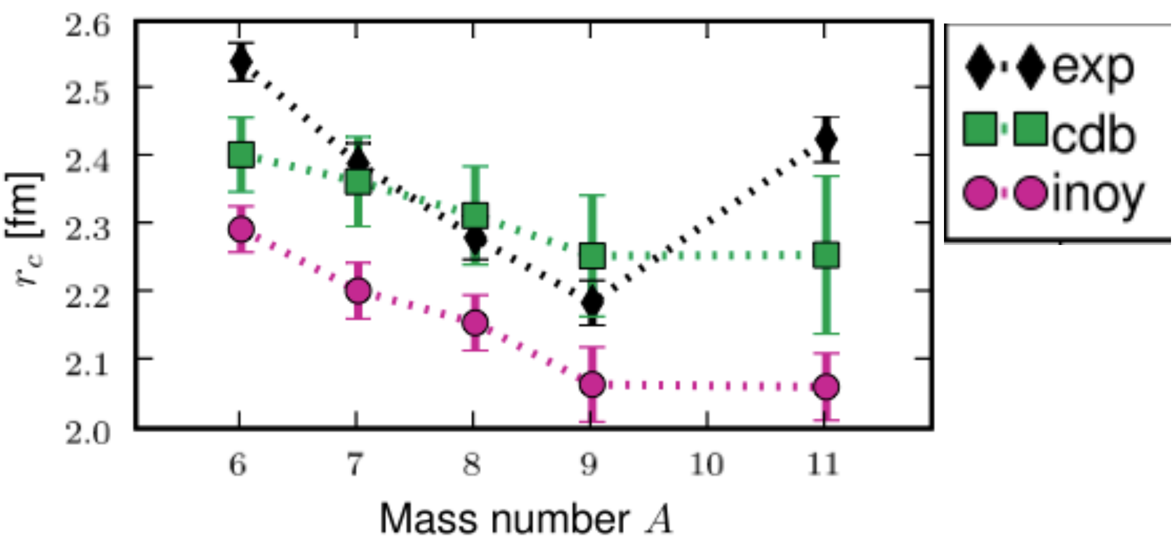

C. Forssen,E. Caurier, P. Navratil, PRC 79 021303 (2009)

Table 2

Data	Value	Refs.
S_{2n}	378 ± 5, 369.15 ± 0.65 keV	[7,8]
^{11}Li matter radius	3.27 ± 0.24, 3.12 ± 0.16, 3.55 ± 0.10 fm	[9–11]
^{9}Li matter radius	2.30 ± 0.02 fm	[10,12]
^{11}Li charge radius	2.467(37), 2.423(34), 2.426(34) fm	[13–15]
^{9}Li charge radius	2.217(35), 2.185(33) fm	[13,14]

To what extent is this picture correct?

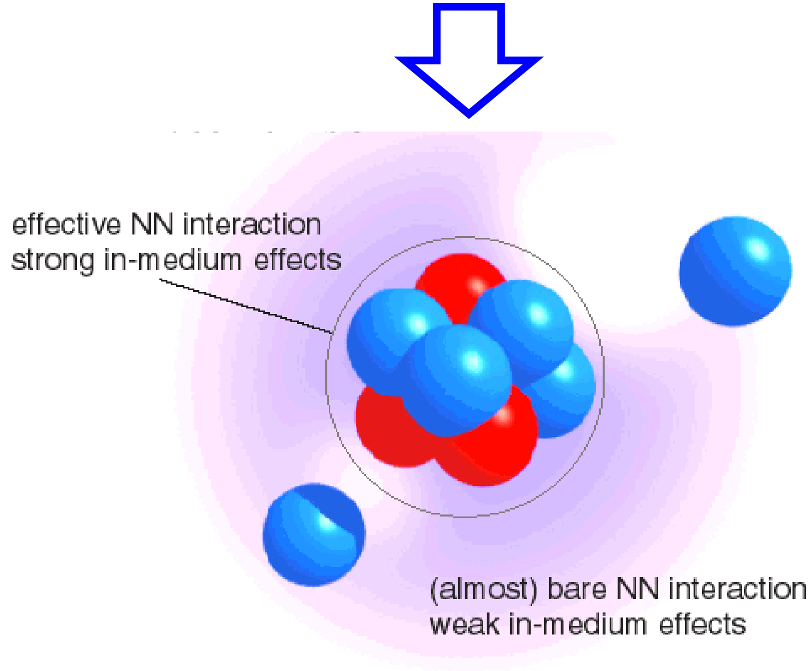

Talk by K. Hagino DCEN 2011

A GENERALIZATION OF THE INERT CORE MODEL

Three-body model with density-dependent delta force

G.F. Bertsch and H. Esbensen,
Ann. of Phys. 209('91)327
H. Esbensen, G.F. Bertsch, K. Hencken,
Phys. Rev. C56('99)3054

^{11}Li, ^{6}He

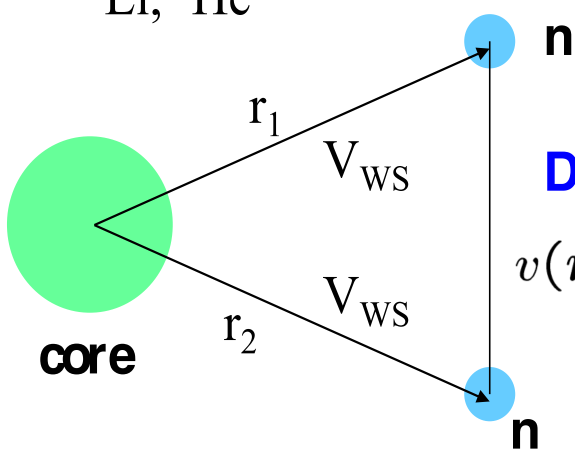

Density-dependent delta-force

$$v(\boldsymbol{r}_1,\boldsymbol{r}_2) = v_0(1+\alpha\rho(r)) \times\delta(\boldsymbol{r}_1-\boldsymbol{r}_2)$$

$$H=\frac{\boldsymbol{p}_1^2}{2m}+\frac{\boldsymbol{p}_2^2}{2m}+V_{nC}(r_1)+V_{nC}(r_2)+V_{nn}+\frac{(\boldsymbol{p}_1+\boldsymbol{p}_2)^2}{2A_cm}$$

... WE INCLUDE CORE SURFACE DYNAMICS: CORE POLARIZATION

AND CORE FLUCTUATIONS :

$$H = p^2_1/2m + p^2_2/2m + V_{nc}(r_1) + V_{nc}(r_2) + V_{nn}(r_{12}) + (\mathbf{p}_1+\mathbf{p}_2)^2/(2A\_c\ m) +$$

$$\delta V_{nc}(r_1,\theta_1,\varphi_1,\{\alpha_{\lambda\mu}\}) \quad + \quad \delta V_{nc}(r_2,\theta_2,\varphi_2,\{\alpha_{\lambda\mu}\}) + H_{coll}$$

where δV_{nc} is the change in V_{nc} due to (core) surface-like deformation $\{\alpha_{\lambda\mu}\}$:

$$\boxed{\delta V_{nc}(r,\theta,\varphi,\{\alpha_{\lambda\mu}\}) = - \Sigma_{\lambda\mu}\ r * dV_{nc}/dr * Y_{\lambda\mu}(\theta,\varphi) * \alpha_{\lambda\mu}}$$

where, for example, $\alpha_{2\mu}$ is the dynamical quadrupole deformation of the core, described (harmonic oscillator formalism) in terms of creation and annihilation of surface oscillation quanta

$$\alpha_{\lambda\mu} = \beta_\lambda (2\lambda+1)^{1/2}(\Gamma^+_{\lambda-\mu} + \Gamma_{\lambda\mu}) \quad ; \quad H_{coll} = \Sigma_{\lambda\mu} (\Gamma^+_{\lambda\mu}\Gamma_{\lambda\mu} + ½)\, \hbar\omega_\lambda$$

β_λ is determined from experiment (inelastic scattering or $B(E\lambda)$), analyzed via a RPA calculation with a **multipole-multipole** force

Parity inversion in N=7 isotones

Experimental systematics

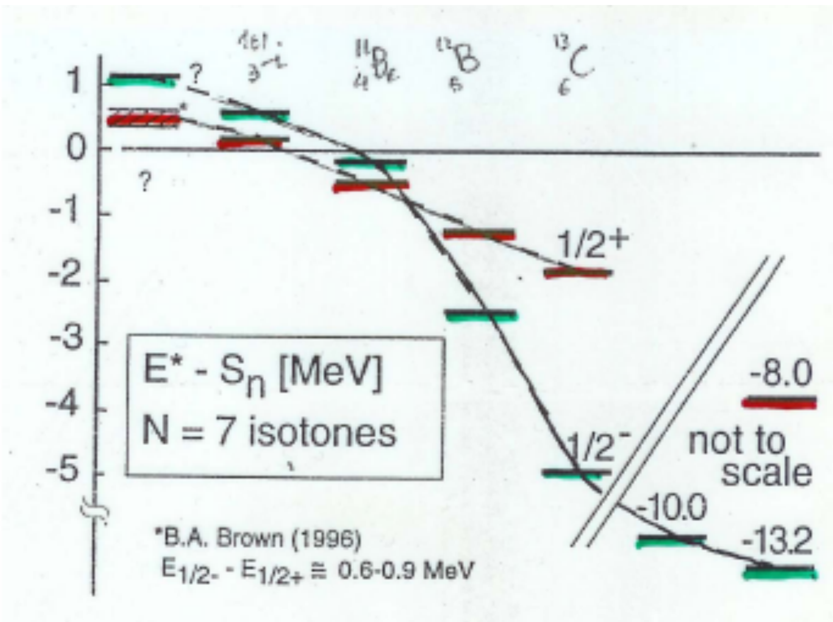

Typical mean-field results

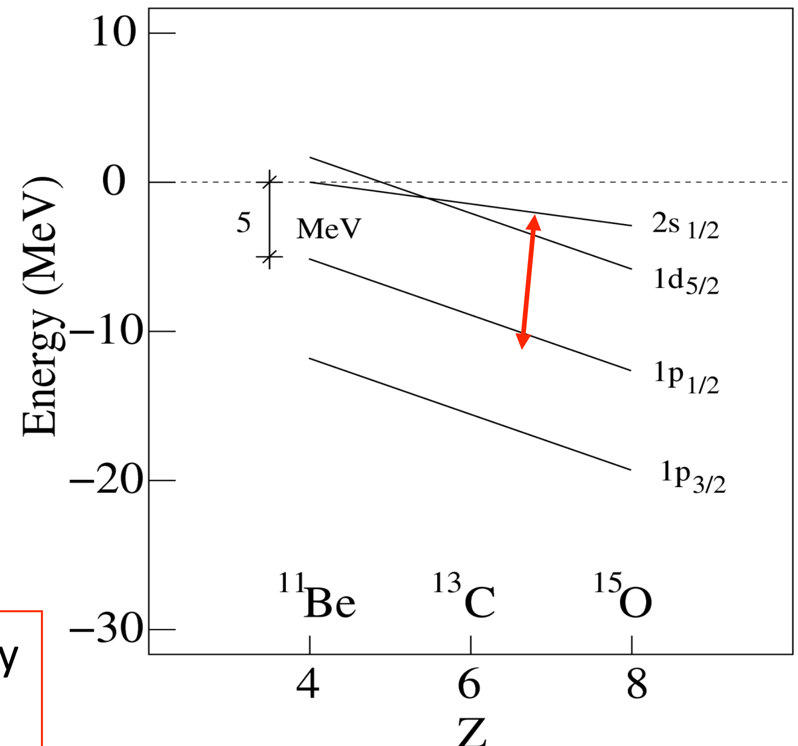

If one ignores core-polarizability/deformability

$$H = p^2_1/2m + V_{nc}(r_1) + (\mathbf{p}_1)^2/(2A\_c\, m) + \cancel{\delta V_{nc}(r_1,\theta_1,\varphi_1,\{\alpha_{\lambda\mu}\})}$$

$$\downarrow$$

A different V_{nc}(r) is needed for each parity

Let us now consider the effects of $\delta V_{nc}(r_1,\theta_1,\varphi_1,\{\alpha_{\lambda\mu}\})$ on the self-energy

1/2- Eshift = - 2.5 MeV

Self-energy

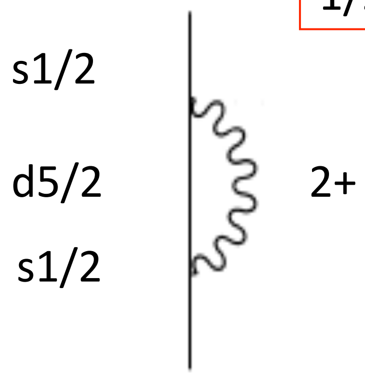

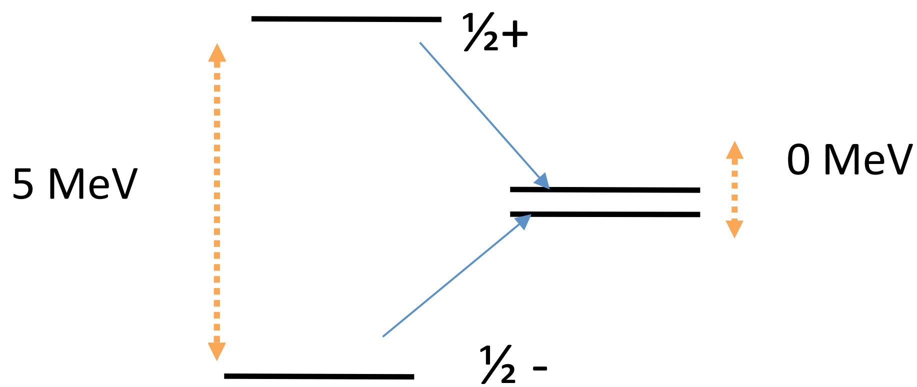

+

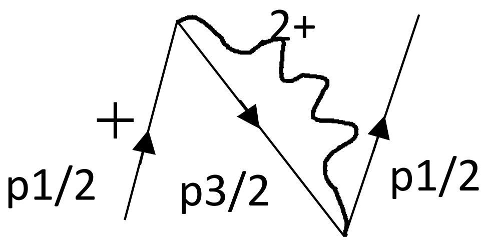

1/2- Eshift = + 2.5 MeV

Pauli blocking of core ground state correlations

H. Sagawa et al., PLB 309 (1993)1

Ground State Correlation Energy and Pauli Blocking

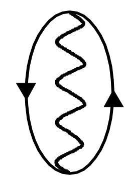

< 0

(a)

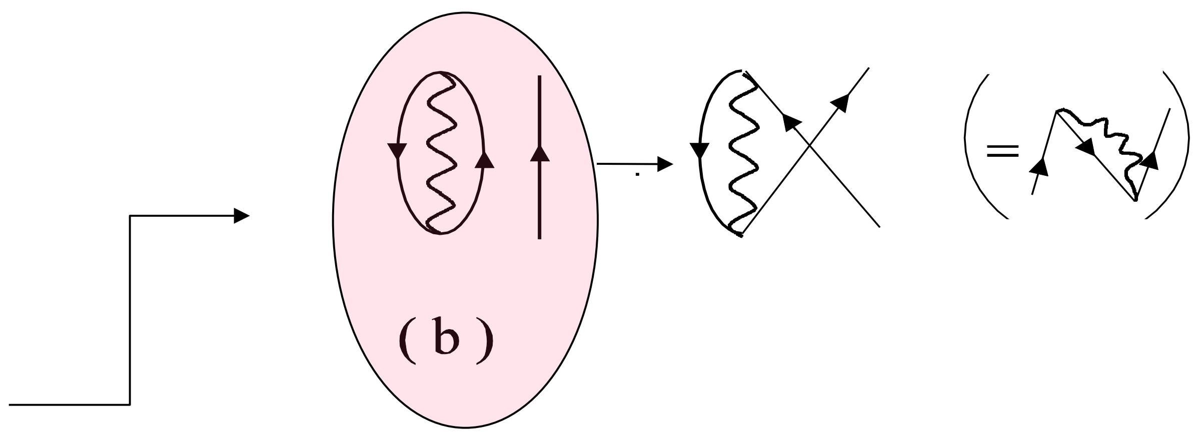

> 0

Forbidden if both particles have the same quantum numbers

ELIMINATE !

(e)

Relax some of the assumptions of the inert core model:

Inert core

Different potentials for s- and p- waves

Zero range interaction, with ad hoc density dependence

Low-lying collective modes of the core taken into account

Standard mean field potential

Bare N-N interaction (Argonne)

H. Esbensen, G.F. Bertsch, K. Hencken, Phys. Rev. C 56 (1997) 3054

^{10}Li, ^{11}Li F. Barranco et al. EPJ A11 (2001) 385
^{11}Be, ^{12}Be G. Gori et al. PRC 69 (2004) 041302(R)

Self-energy matrix in the discretized continuum

^{11}Be

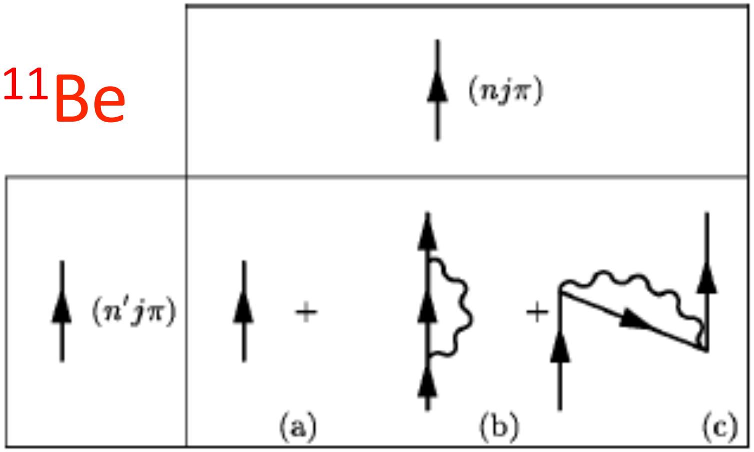

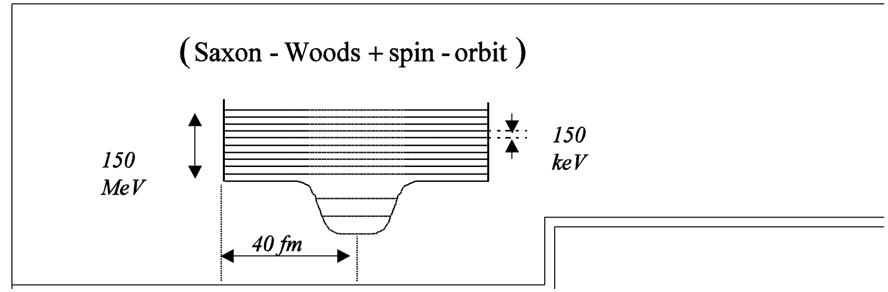

Main ingredients of our calculation

Fermionic degrees of freedom:

• s1/2, p1/2, d5/2 Wood-Saxon levels up to 150 MeV (discretized continuum) from a standard (Bohr-Mottelson) Woods-Saxon potential

Bosonic degrees of freedom:

• 2+ and 3- QRPA solutions with energy up to 50 MeV; residual interaction: multipole-multipole separable with the coupling constant tuned to reproduce E(2+)=3.36 MeV and $0.6<\beta_2<0.7$

Admixture of $d_{5/2}$ x 2^+ configuration in the $1/2^+$ g.s. of ^{11}Be is about 20%

Calculated ground state

$$|1/2+\rangle = \sqrt{0.87}\,|s_{1/2}\rangle + \sqrt{0.13}\,|d_{5/2}\otimes 2+\rangle$$

Exp.:

J.S. Winfield et al., Nucl.Phys. **A683** (2001) 48

$$|1/2+\rangle = \sqrt{0.84}\,|s_{1/2}\rangle + \sqrt{0.16}\,|d_{5/2}\otimes 2+\rangle$$

$^{11}Be(p,d)^{10}Be$ in inverse kinematic detecting both the ground state and the 2+ excited state of ^{10}Be.

9Be(11Be,10Be+ γ) X

T. Aumann et al.
PRL 84(2000)35

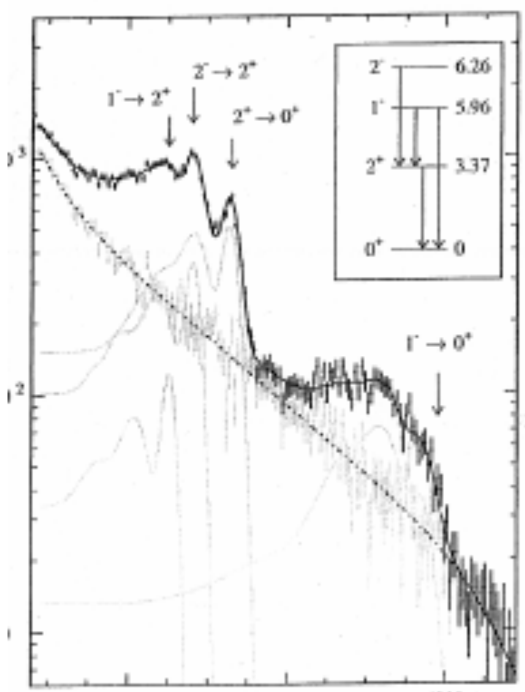

p(11Be,10Be)d

S. Fortier et al.
Phys. Lett.B461(1999)22

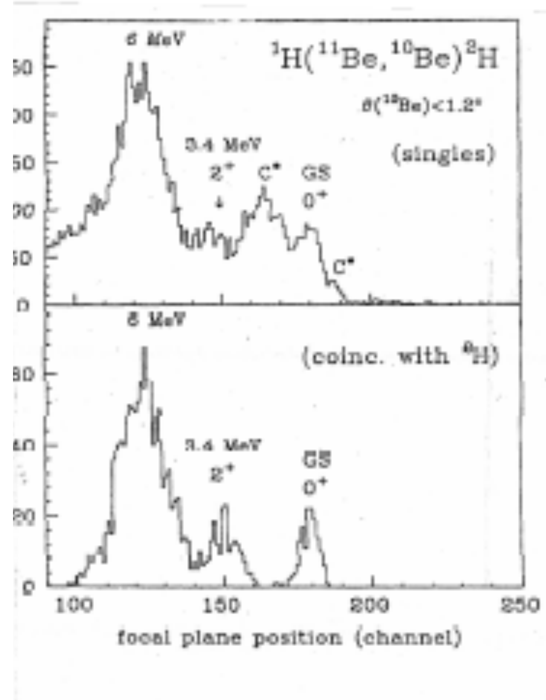

Good agreement also between theory and experiment concerning energies and "spectroscopic" factors in 12Be

New result for S[1/2+]: $0.28^{+0.03}_{-0.07}$

Kanungo et al.
PLB 682 (2010) 39

Spectroscopic factors from (12Be,11Be+γ) reaction to ½⁺ and ½- final states:
S[1/2-]= 0.37±0.10 S[1/2+]= 0.42±0.10

A. Navin et al.,
PRL 85(2000)266

			Theory	
		Expt.	Particle vibration	Mean field
$^{11}_{4}Be_7$	$E_{s_{1/2}}$	−0.504 MeV	−0.48 MeV	~0.14 MeV
	$E_{p_{1/2}}$	−0.18 MeV	−0.27 MeV	−3.12 MeV
	$E_{d_{5/2}}$	1.28 MeV	~0 MeV	~2.4 MeV
	$S[1/2^+]$	0.65−0.80 [19]	0.87	1
		0.73±0.06 [20]		
		0.77 [21]		
	$S[1/2^-]$	0.63±0.15 [20]	0.96	1
		0.96 [21]		1
	$S[5/2^+]$		0.72	1
$^{12}_{4}Be_8$	S_{2n}	−3.673 MeV	−3.58 MeV	−6.24 MeV
	s^2,p^2,d^2		23%, 29%, 48%	0%, 100%, 0%
	$S[1/2^+]$	0.42±0.10 [7]	0.31	0
	$S[1/2^-]$	0.37±0.10 [7]	0.57	2

Good agreement between theory and experiment concerning energies and spectroscopic factors in ^{11}Be

			Theory	
		Expt.	Particle vibration	Mean field
	$E_{s_{1/2}}$	−0.504 MeV	−0.48 MeV	~0.14 MeV
	$E_{p_{1/2}}$	−0.18 MeV	−0.27 MeV	−3.12 MeV
$^{11}_{4}\mathrm{Be}_7$	$E_{d_{5/2}}$	1.28 MeV	~0 MeV	~2.4 MeV
	$S[1/2^+]$	0.65−0.80 [19]	0.87	1
		0.73±0.06 [20]		
		0.77 [21]		
	$S[1/2^-]$	0.63±0.15 [20]	0.96	1
		0.96 [21]		1
	$S[5/2^+]$		0.72	1

^{10}Li results

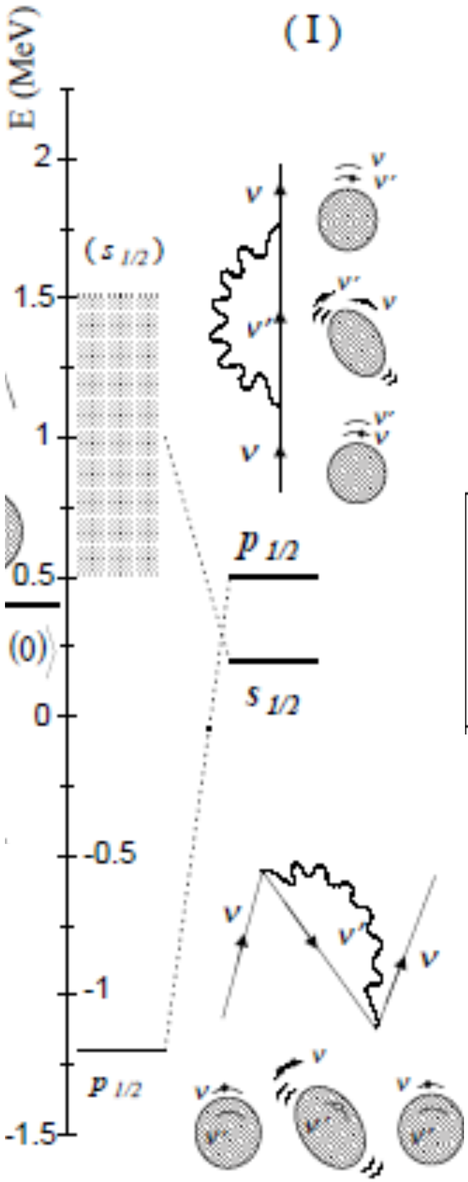

		Exp.	Theory	
			particle-vibration +Argonne	mean field
$^{10}_{3}Li_7$ (not bound)	s	0.1-0.2 MeV	0.2 MeV (virtual)	$\sim$ 1 MeV (virtual)
	p	0.5-0.6 MeV	0.5 MeV (res.)	-1.2 MeV (bound)

A dynamical description of two-neutron halos

Diagonalization of H_{eff} (E)

^{11}Li
F. Barranco et al. EPJ A11 (2001) 385

^{12}Be
G. Gori et al. PRC 69 (2004) 041302(R)

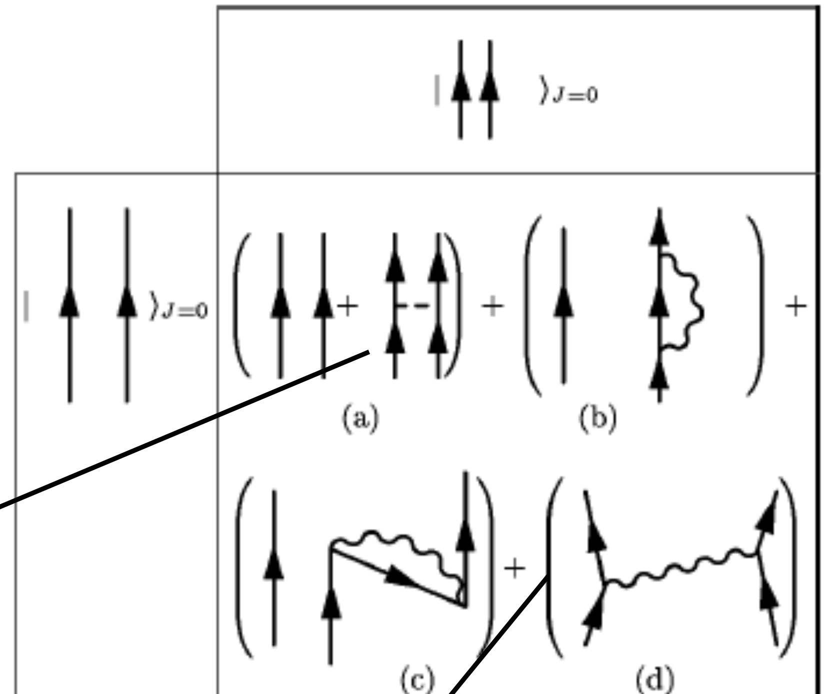

Bare interaction

Induced interaction

Quadr.

Table 2. RPA wave function of the collective low-lying quadrupole phonon in ^{11}Li, of energy $E_{2^+} = 5.05$ MeV, and leading to the most important contribution to the induced interaction in fig. 1, II. All the listed amplitudes refer to neutron transitions, except for the last column. We have adopted the self-consistent value ($\chi_2 = 0.013\,\mathrm{MeV}^{-1}$) for the coupling constant. The resulting value for the deformation parameter is $\beta_2 = 0.5$.

	$1p_{3/2}^{-1}1p_{1/2}$	$2s_{1/2}^{-1}5d_{3/2}$	$1p_{1/2}^{-1}6p_{3/2}$	$2s_{1/2}^{-1}3d_{5/2}$	$2s_{1/2}^{-1}5d_{5/2}$	$1p_{3/2}^{-1}1p_{1/2}$ (π)
X_{ph}	0.824	0.404	0.151	0.125	0.126	0.16
Y_{ph}	0.119	0.011	−0.002	−0.049	−0.011	0.07

B(E1) calculated with separable force; coupling constant tuned to reproduce experimental strength; part of the strength comes from admixture of GDR

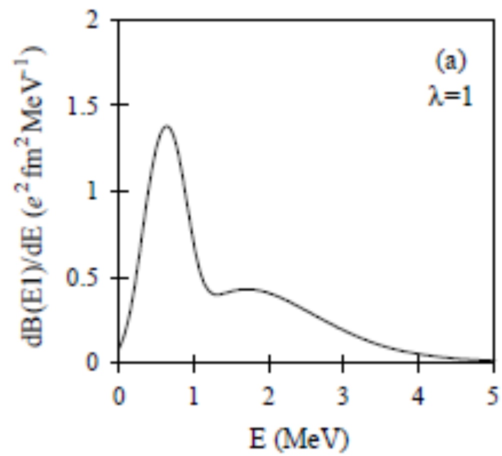

Table 3. RPA wave function of the strongest low-lying dipole vibration of ^{11}Li, ($E_{1^-} = 0.75$ MeV), and contributing most importantly to the pairing induced interaction (fig. 1, II). All the listed amplitudes refer to neutron transitions. We have used the value $\chi_1 = 0.0043\,\mathrm{MeV}^{-1}$ for the isovector coupling constant in order to get a good agreement with the experimental findings. To be noted that this value coincides within 25% close to the selfconsistent value of $0.0032\,\mathrm{MeV}^{-1}$. The resulting strength function (cf. fig. 2(a)) integrated up to 4 MeV gives 7% of the Thomas-Reiche-Kuhn energy weighted sum rule, to be compared to the experimental value of 8% [38].

Soft dipole

	$1p_{1/2}^{-1}2s_{1/2}$	$1p_{1/2}^{-1}3s_{1/2}$	$1p_{1/2}^{-1}4s_{1/2}$	$1p_{1/2}^{-1}1d_{3/2}$	$1p_{3/2}^{-1}5d_{5/2}$	$1p_{3/2}^{-1}6d_{5/2}$	$1p_{3/2}^{-1}7d_{5/2}$
X_{ph}	0.847	−0.335	0.244	0.165	0.197	0.201	0.157
Y_{ph}	0.088	0.060	0.088	0.008	0.165	0.173	0.138

Valence transitions

Core transitions

Theoretical calculation for ^{11}Li

Low-lying dipole strength

↓

s-p strong mixing

also

Strong Pauli correction is needed:

About 50% in each vertex

The recoil term p1*p2/AM is incorporated as a dipole-dipole term

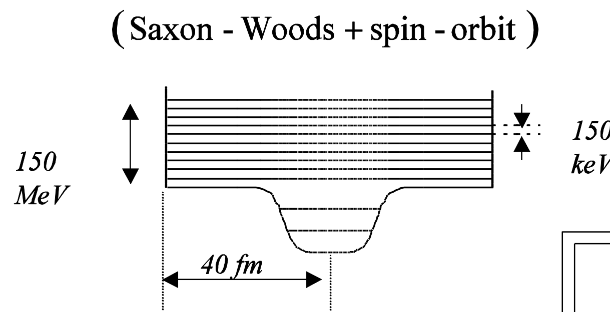

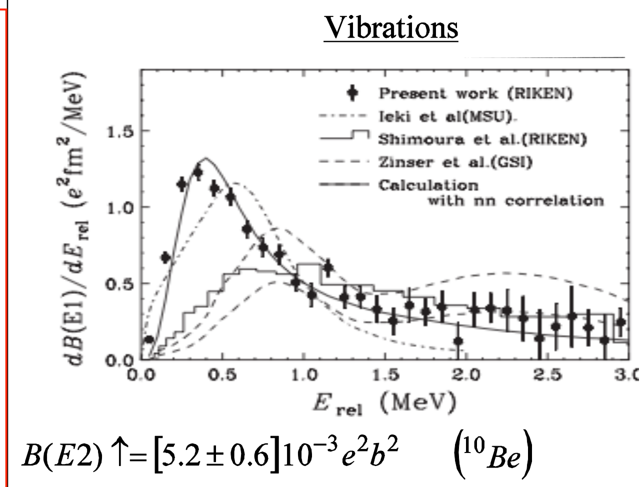

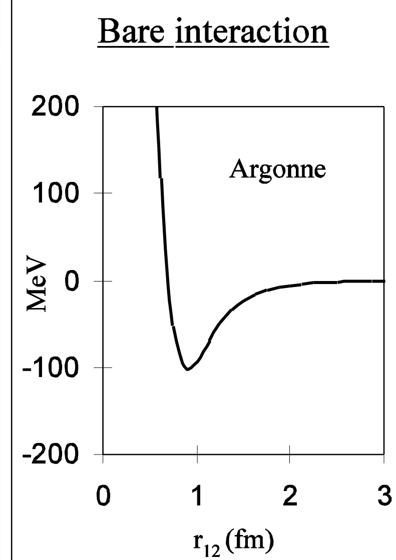

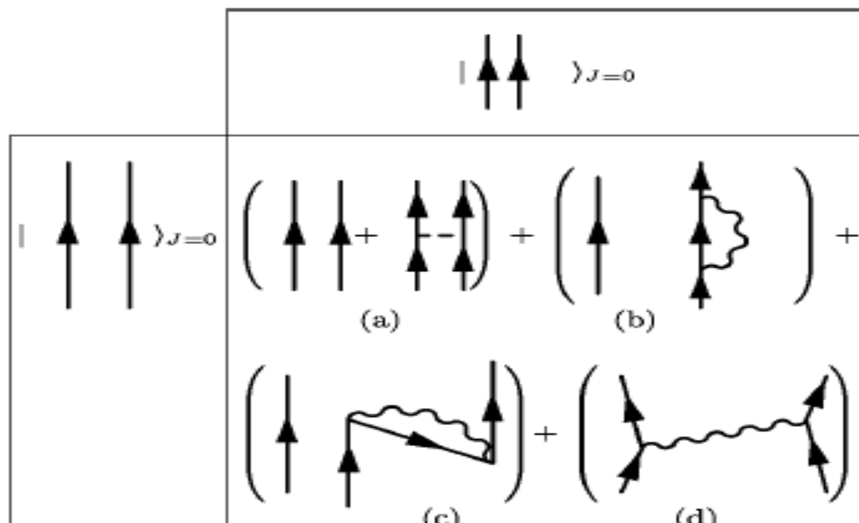

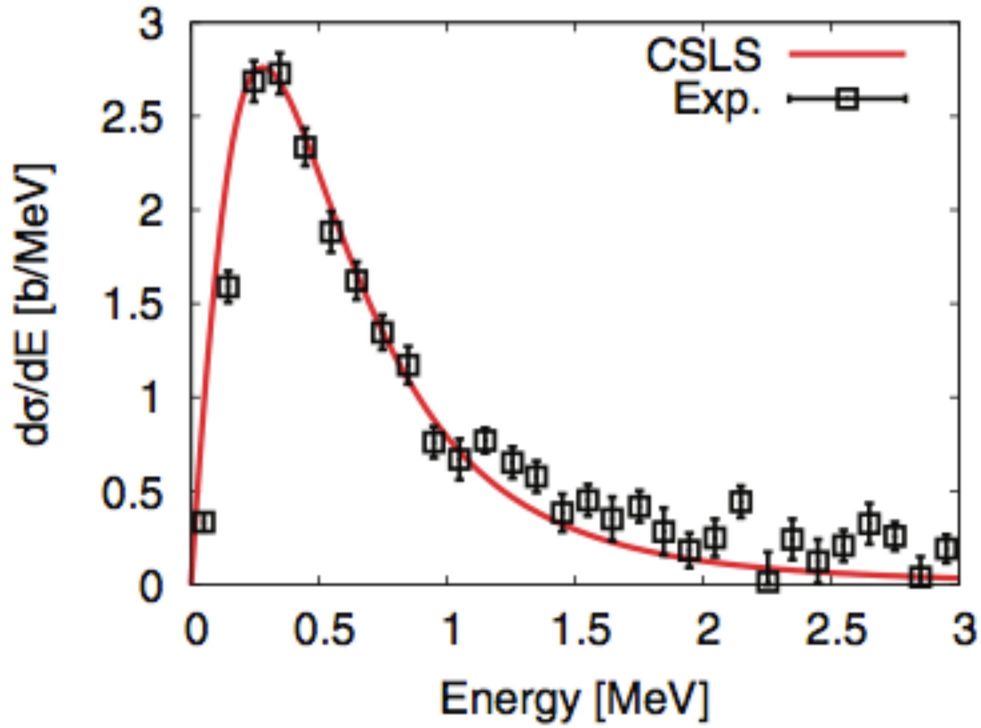

The excitation of the ^{9}Li core is also important to reproduce the total breakup strength, because about 15% of the strength escapes to the higher energy region as the component of the core excitation in the present coupled-channel approach. This

Y. Kikuchi et al., PRC 87 ,034606 (2013)

^{10}Li and ^{11}Li results

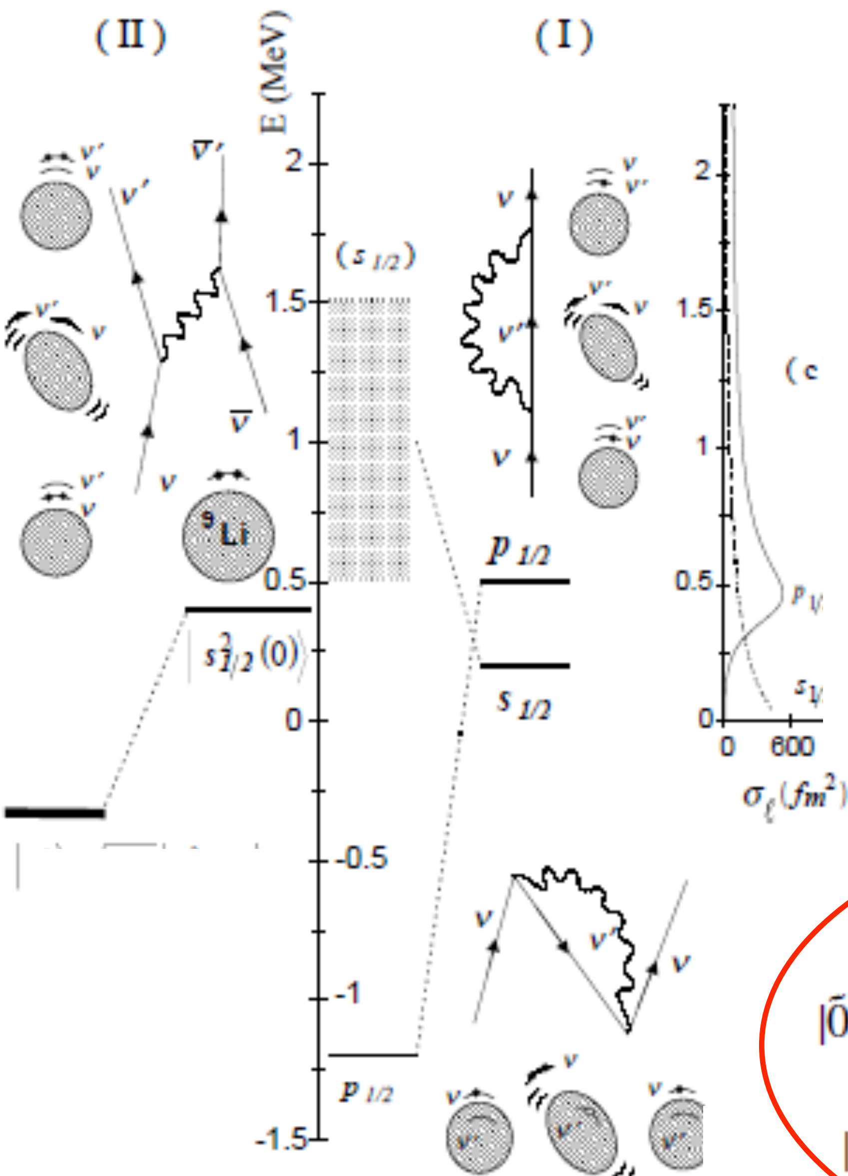

		Exp.	Theory	
			particle-vibration +Argonne	mean field
$^{10}_{3}$Li$_7$ (not bound)	s	0.1-0.2 MeV	0.2 MeV (virtual)	~ 1 MeV (virtual)
	p	0.5-0.6 MeV	0.5 MeV (res.)	-1.2 MeV (bound)
$^{11}_{3}$Li$_8$ (bound)	S_{2n}	0.369 MeV	0.33 MeV	2.4 MeV
	s^2, p^2	50% , 50%	41% , 59%	0% , 100%
	$\langle r^2\rangle^{1/2}$	3.55±0.1 fm	3.9 fm	
	$\Delta p_\perp$	48±10 MeV/c	55 MeV/c	

11Li correlated wave function

$$|\tilde{0}\rangle = |0\rangle + 0.7|(ps)_{1^-} \otimes 1^-; 0\rangle + 0.1|(sd)_{2^+} \otimes 2^+; 0\rangle$$

$$|0\rangle = 0.45|s^2_{1/2}(0)\rangle + 0.55|p^2_{1/2}(0)\rangle + 0.04|d^2_{5/2}(0)\rangle$$

Correlated halo wavefunction

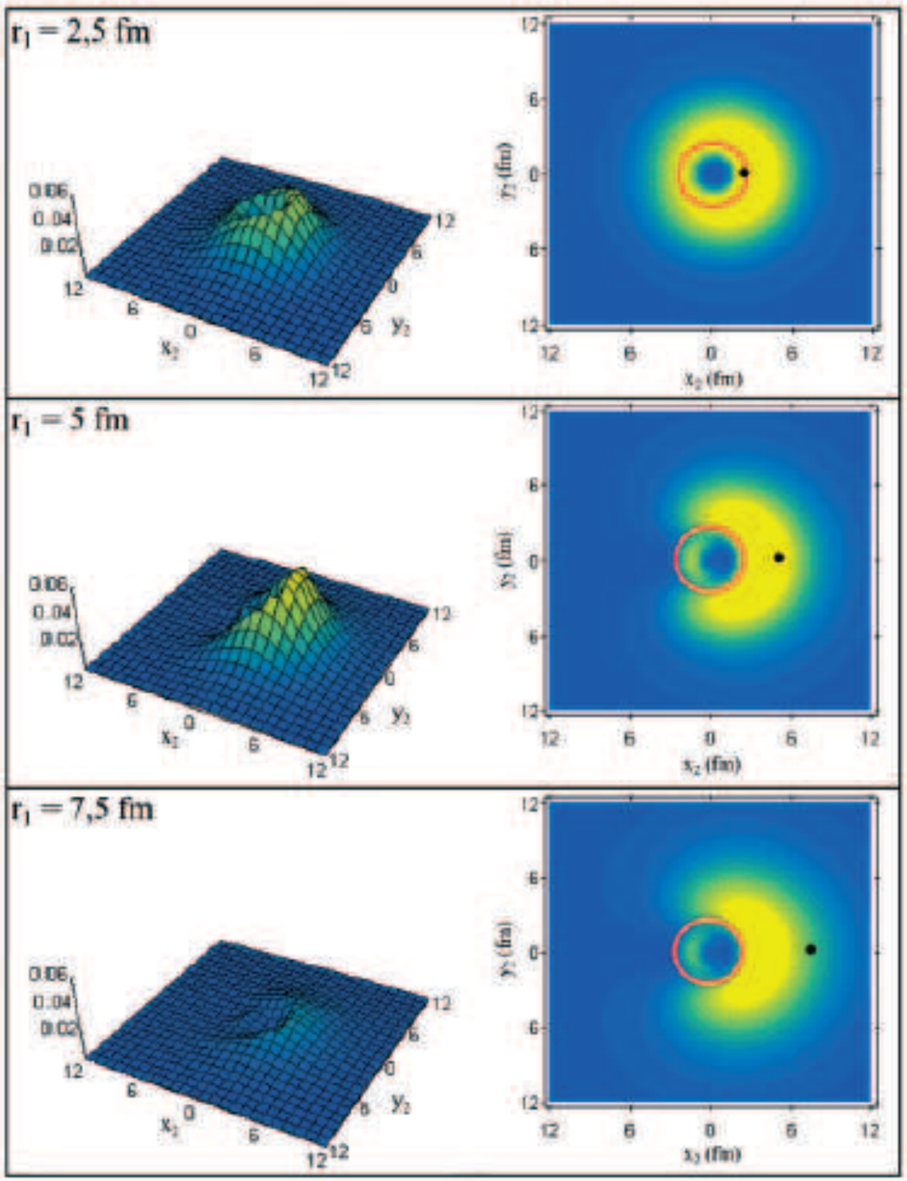

Uncorrelated

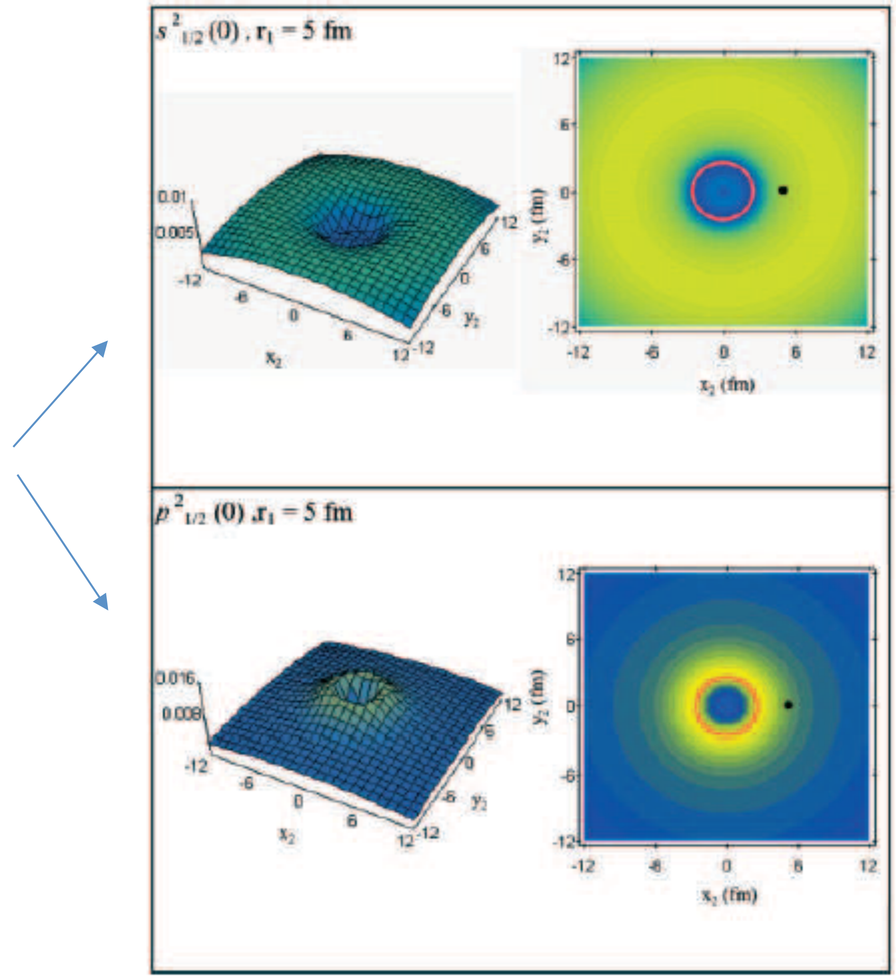

Role of coupling to continuum

11Li correlated wave function

$$|\tilde{0}\rangle = |0\rangle + 0.7|(ps)_{1^-} \otimes 1^-; 0\rangle + 0.1|(sd)_{2^+} \otimes 2^+; 0\rangle$$

$$|0\rangle = 0.45|s^2_{1/2}(0)\rangle + 0.55|p^2_{1/2}(0)\rangle + 0.04|d^2_{5/2}(0)\rangle$$

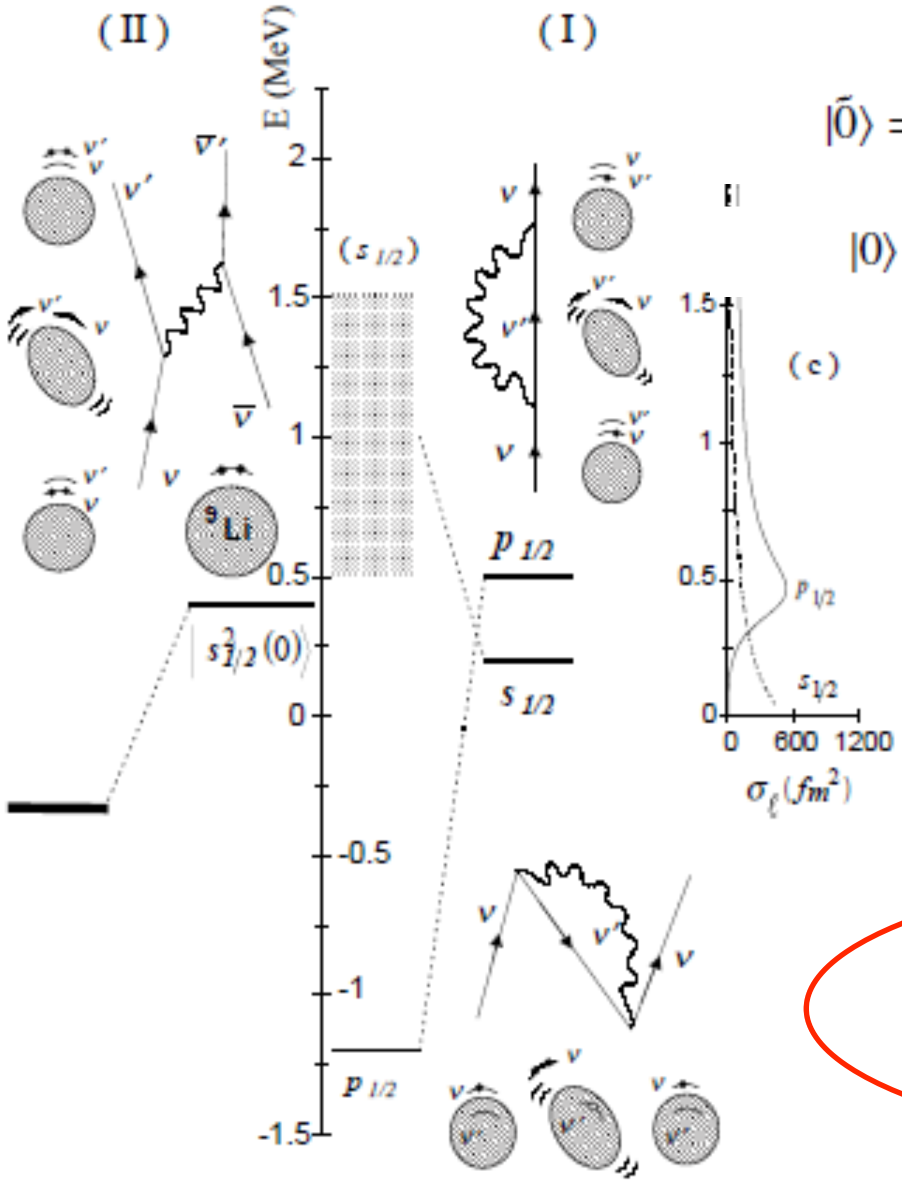

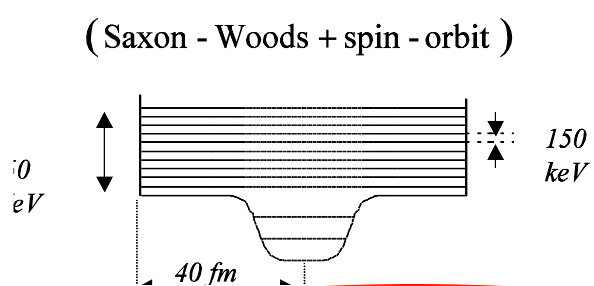

Mixing n/n' ($[\varphi_{nlj} \times \varphi_{n'lj}]0+$) in the continuum creates bound waves

Comparison with the model by Bertsch and Esbensen

OUR MODEL

Ann. Phys.209(1991)327
PRC56(1997)3054

Single-particle potential

Parity independent potential (Bohr-Mottelson)

f

Depth adjusted to experimental $p_{1/2}$ single particle energy

2-body interaction

Bare Argonne interaction+ particle-vibration coupling with phenomenological parameters (low-lying vibrations)

Strength fitted to S_{2n} in ^{12}Be

$$v_{\text{eff}}(\mathbf{r}_1,\mathbf{r}_2)=\delta(\mathbf{r}_1-\mathbf{r}_2)\left(v_0+v_\rho\left(\frac{\rho_c((\mathbf{r}_1+\mathbf{r}_2)/2)}{\rho_0}\right)^P\right).$$

Results

Good reproduction of binding energies in ^{12}Be and ^{11}Li
50% $(s_{1/2})^2$

Good reproduction of binding energy
Low $(s_{1/2})^2$ admixture unless two different s.p. potentials are used

Comparison with the model by Ikeda, Myo et al.

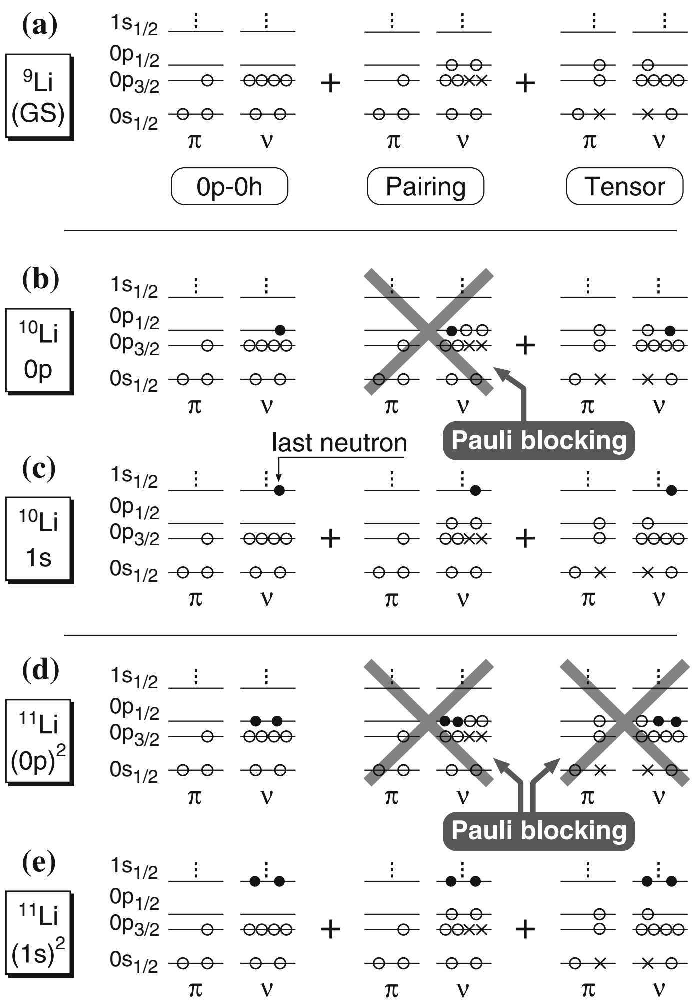

K. Ikeda et al,
Lect. Notes in Physics 818 (2010)

$p_{1/2}$ orbit is pushed up by pairing correlations
and tensor force. Only 3/2- configurations
are included: coupling to core vibrations (1/2-) is
not considered. Binding energy is given as input. 50%(s^2)-50%(p^2) wavefunction is obtained

How to probe the particle-phonon coupling?
Test the microscopic correlated wavefunction with phonon admixture

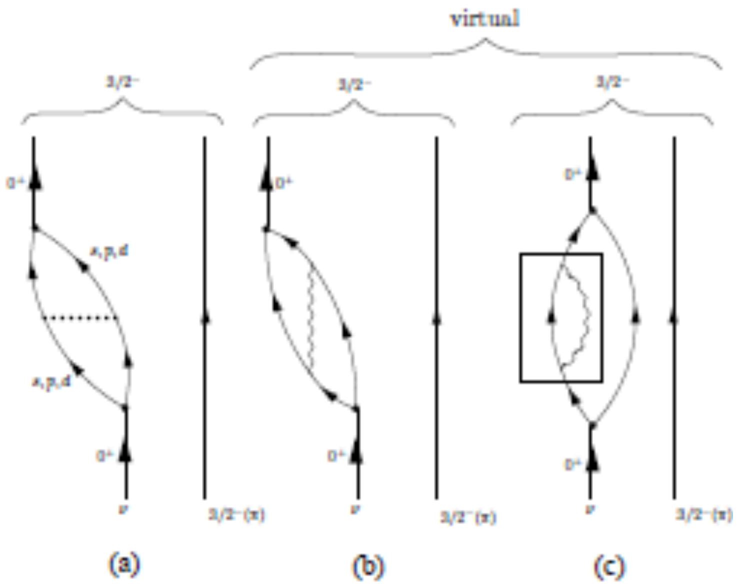

$$|\tilde{0}\rangle = |0\rangle + 0.7|(ps)_{1^-} \otimes 1^-;0\rangle + 0.1|(sd)_{2^+} \otimes 2^+;0\rangle$$

$$|0\rangle = 0.45|s^2_{1/2}(0)\rangle + 0.55|p^2_{1/2}(0)\rangle + 0.04|d^2_{5/2}(0)\rangle$$

Two-neutron transfer to

ground state

exc. state

We will try to draw information about the halo structure of ^{11}Li from the reactions ^{1}H(^{11}Li,^{9}Li)^{3}H and ^{1}H(^{11}Li,^{9}Li*(2.69 MeV))^{3}H (I. Tanihata *et al.*, Phys. Rev. Lett. **100**, 192502 (2008))

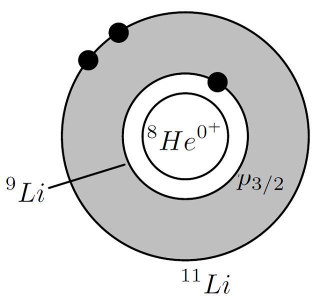

Schematic depiction of ^{11}Li

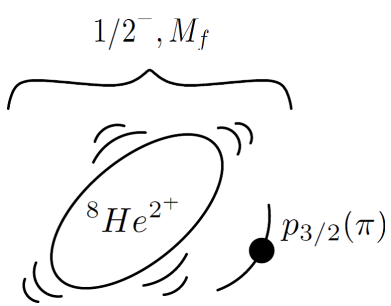

First excited state of ^{9}Li

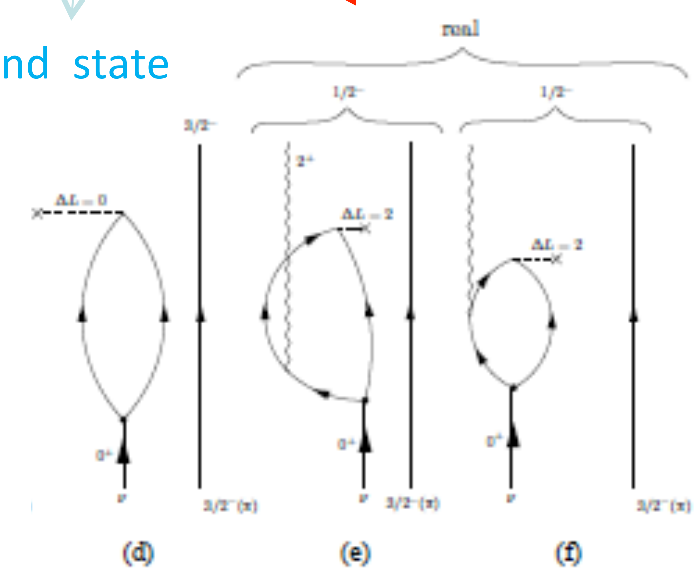

Probing ^{11}Li halo-neutrons correlations via (p,t) reaction

PRL **100,** 192502 (2008) PHYSICAL REVIEW LETTERS week ending 16 MAY 200

Measurement of the Two-Halo Neutron Transfer Reaction ^{1}H(^{11}Li, ^{9}Li)^{3}H at 3*A* MeV

I. Tanihata,* M. Alcorta,† D. Bandyopadhyay, R. Bieri, L. Buchmann, B. Davids, N. Galinski, D. Howell, W. Mills, S. Mythili, R. Openshaw, E. Padilla-Rodal, G. Ruprecht, G. Sheffer, A.C. Shotter, M. Trinczek, and P. Walden

TRIUMF, 4004 Wesbrook Mall, Vancouver, BC, V6T 2A3, Canada

H. Savajols, T. Roger, M. Caamano, W. Mittig,‡ and P. Roussel-Chomaz

GANIL, Bd Henri Becquerel, BP 55027, 14076 Caen Cedex 05, France

R. Kanungo and A. Gallant

Saint Mary's University, 923 Robie St., Halifax, Nova Scotia B3H 3C3, Canada

M. Notani and G. Savard

ANL, 9700 S. Cass Ave., Argonne, Illinois 60439, USA

I. J. Thompson

LLNL, L-414, P.O. Box 808, Livermore, California 94551, USA

(Received 22 January 2008; published 14 May 2008)

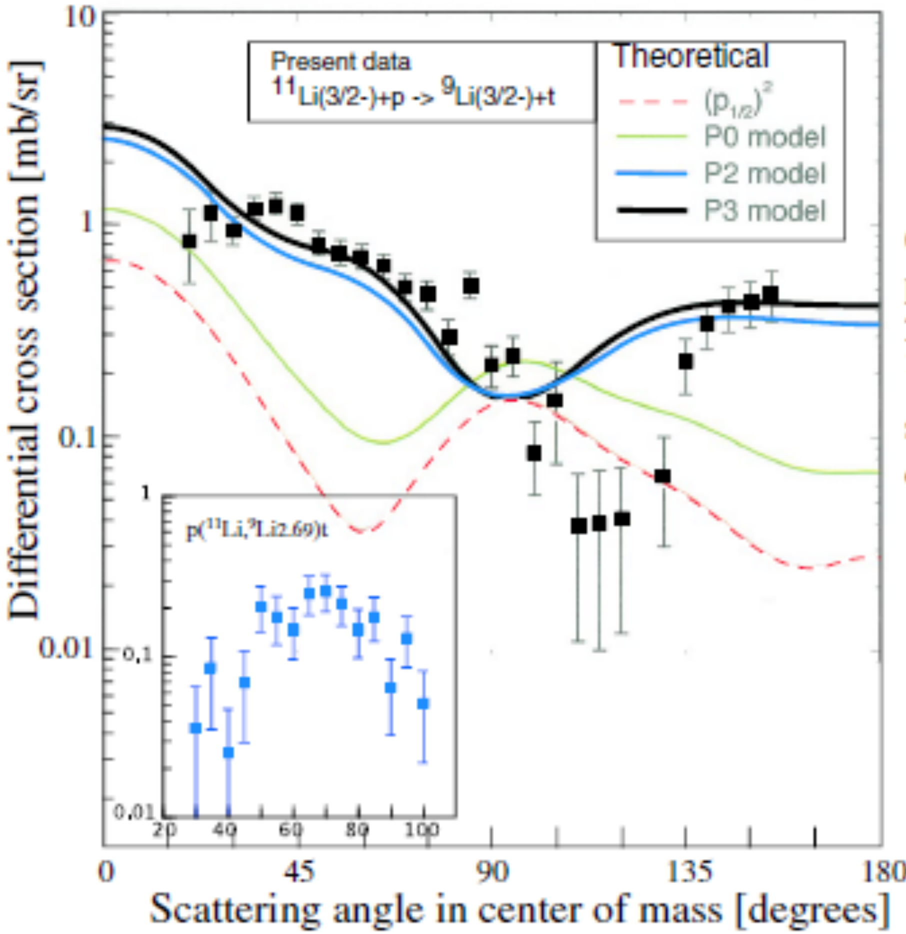

The cross section for transitions to the first excited state (Ex = 2.69 MeV) is shown also in Fig. 3. If this state were populated by a direct transfer, it would indicate that a 1^+ or 2^+ halo component is present in the ground state of ^{11}Li($\frac{3}{2}^-$), because the spin-parity of the ^{9}Li first excited state is $\frac{1}{2}^-$. This is new information that has not yet been observed in any of previous investigations. A compound

TABLE I. Optical potential parameters used for the present calculations.

	V MeV	r_V fm	a_V fm	W MeV	W_D MeV	r_W fm	a_W fm	V_{so} MeV	r_{so} fm	a_{so} fm
$p + {}^{11}$Li [10]	54.06	1.17	0.75	2.37	16.87	1.32	0.82	6.2	1.01	0.75
$d + {}^{10}$Li [11]	85.8	1.17	0.76	1.117	11.863	1.325	0.731	0		
$t + {}^{9}$Li [12]	1.42	1.16	0.78	28.2	0	1.88	0.61	0		

Calculation of absolute two-nucleon transfer cross section by finite-range DWBA calculation

simultaneous and successive contributions

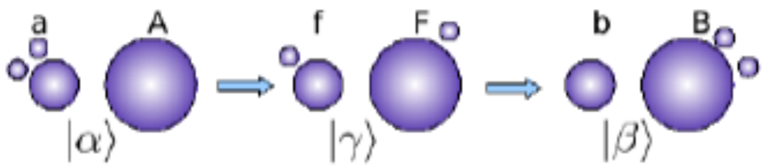

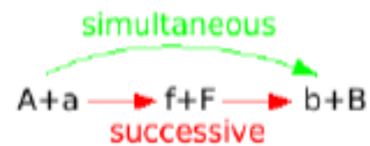

the initial and final channel wave functions are

$$
\begin{aligned}
|\alpha\rangle &= \phi_a(\xi_b, \mathbf{r}_1, \mathbf{r}_2)\phi_A(\xi_A)\chi_{aA}(\mathbf{r}_{aA}) \\
|\beta\rangle &= \phi_b(\xi_b)\phi_B(\xi_A, \mathbf{r}_1, \mathbf{r}_2)\chi_{bB}(\mathbf{r}_{bB})
\end{aligned}
$$

very schematically, the first order (*simultaneous*) contribution is

$$
T^{(1)} = \langle\beta|V|\alpha\rangle,
$$

while the second order contribution can be separated in a *successive* and a *non-orthogonality* term

$$
\begin{aligned}
T^{(2)} &= T^{(2)}_{succ} + T^{(2)}_{NO} \\
&= \sum_\gamma \langle\beta|V|\gamma\rangle G \langle\gamma|V|\alpha\rangle - \sum_\gamma \langle\beta|\gamma\rangle\langle\gamma|V|\alpha\rangle.
\end{aligned}
$$

B.F. Bayman and J. Chen, Phys. Rev. C 26 (1982) 150
M. Igarashi, K. Kubo and K. Yagi, Phys. Rep. 199 (1991) 1
G. Potel et al., arXiv: 0906.4298

$$\sum_{n_1,n_2} a_{n_1,n_2}[\psi_{n_1}(r_1)\psi_{n_2}(r_2)]_{00}$$

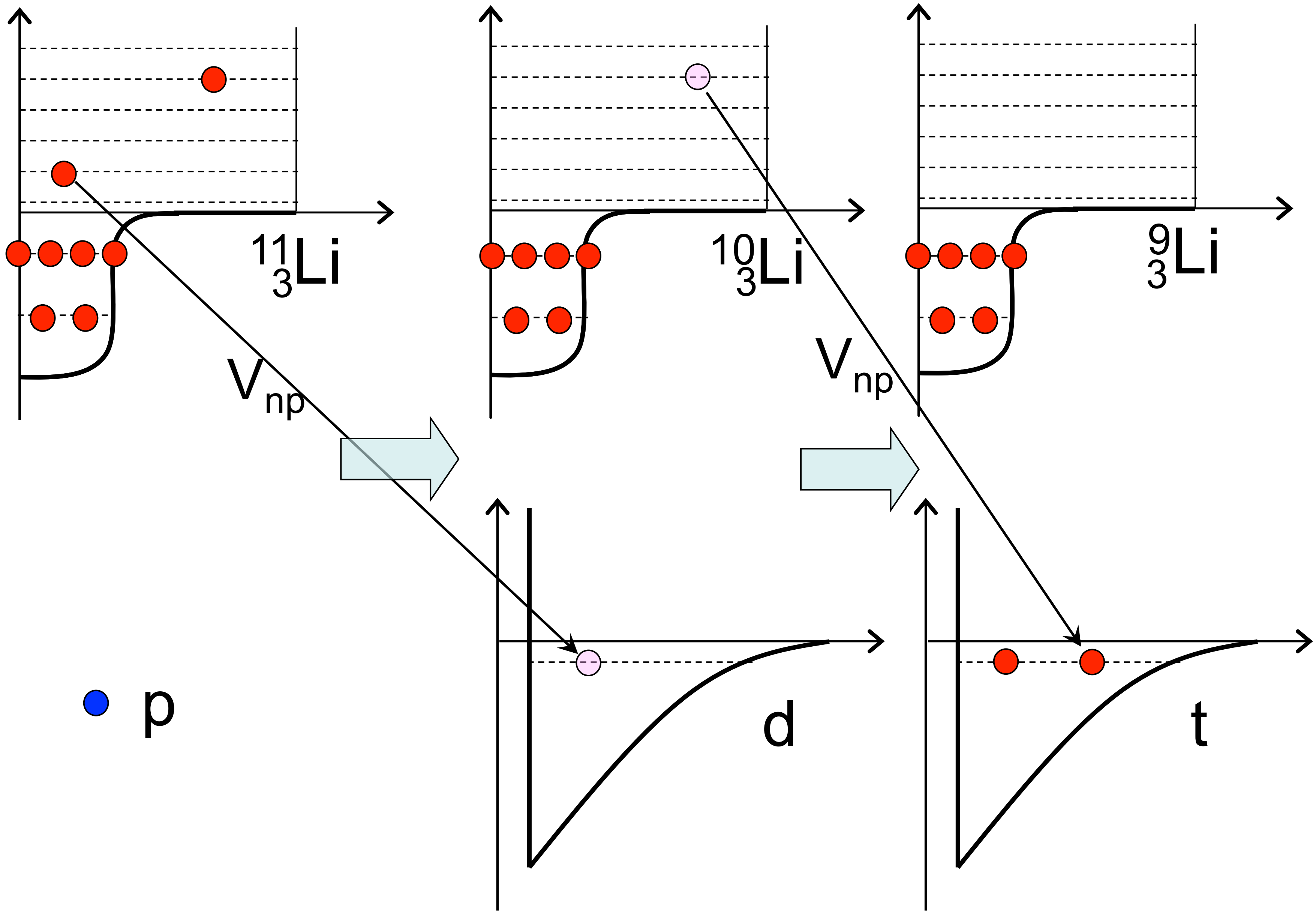

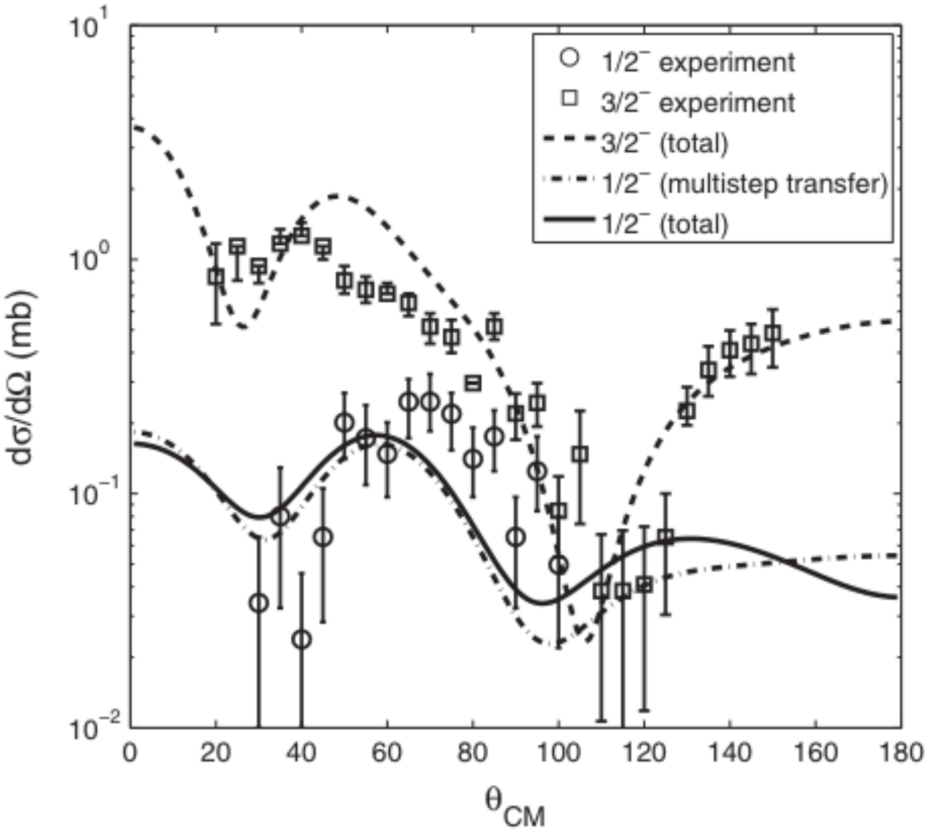

	$\sigma(^{11}\mathrm{Li(gs)} \rightarrow {}^{9}\mathrm{Li\ (i)})$ (mb)		
i	ΔL	Theory	Experiment
gs ($3/2^-$)	0	6.1	5.7 ± 0.9
2.69 MeV ($1/2^-$)	2	0.5	1.0 ± 0.36

G. Potel et al., PRL 105 (2010) 172502

Channels c leading to the first $1/2^-$ excited state of ^{9}Li

$c = 1$: Transfer of the two halo neutrons
$c = 2$: Transfer of a $p_{1/2}$ halo neutron and a $p_{3/2}$ core neutron
$c = 3$: Transfer to the ground state + inelastic excitation

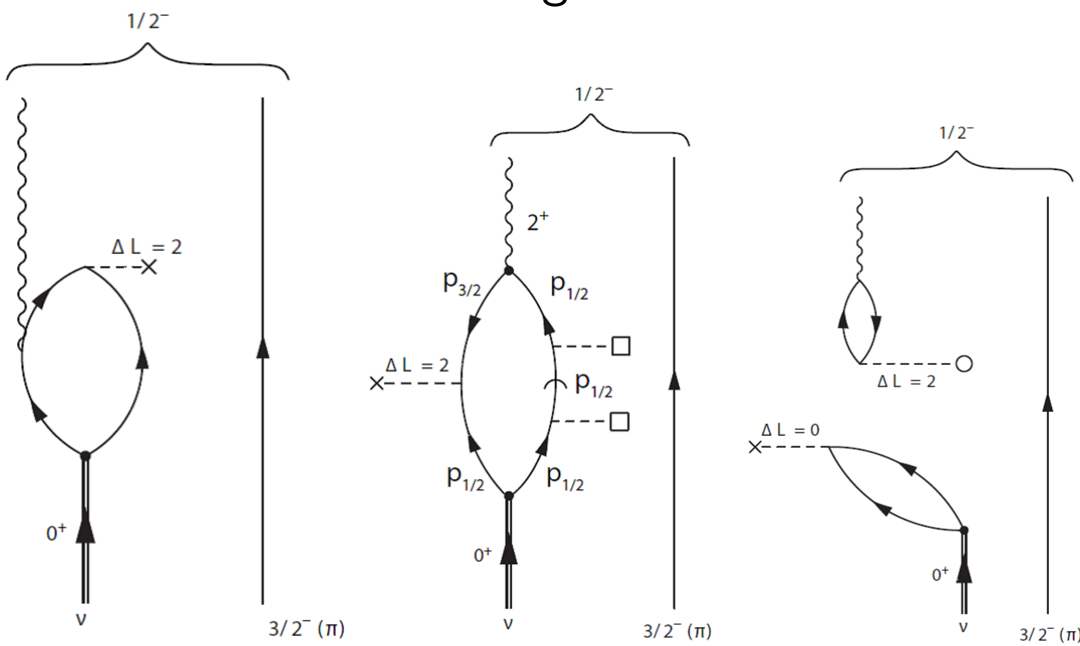

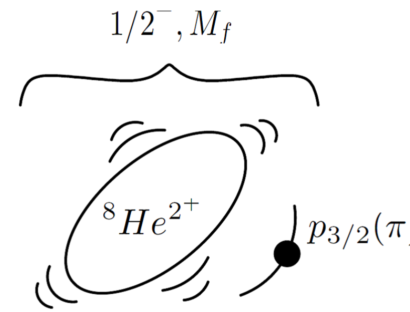

$P^{(1)} = 1.3 \times 10^{-3}$

$P^{(2)} = 4.6 \times 10^{-5}$
$P^{(3)} = 2.6 \times 10^{-6}$

$\sigma_c = \frac{\pi}{k^2} \sum_l (2l+1)|S_l^{(c)}|^2, \; P^{(c)} = \sum_l |S_l^{(c)}|^2 \; (c = 1, 2, 3).$
Small probabilities $\Rightarrow$ use of second order perturbation theory.

Convergence of the calculation

With box radius (30,40 fm)

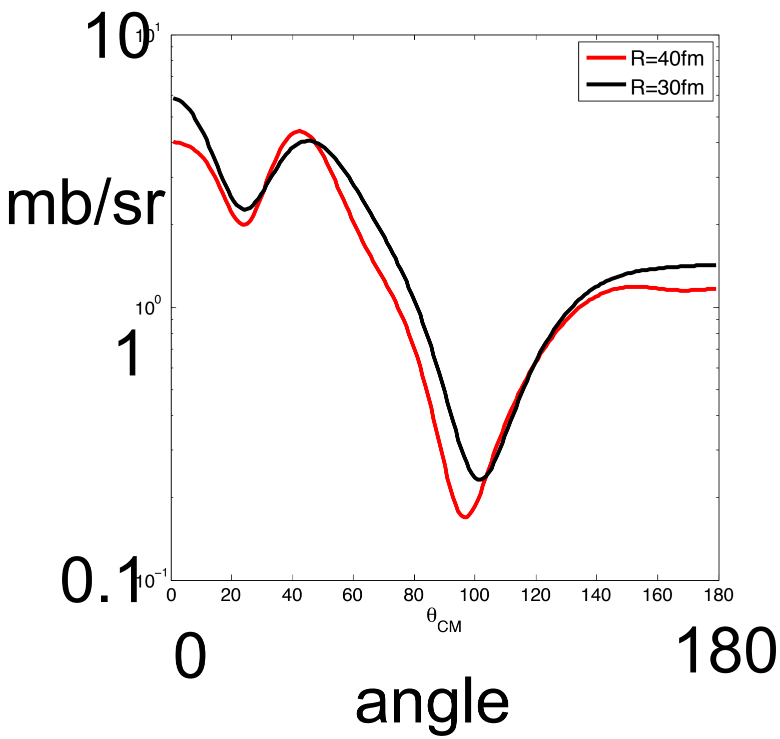

With number of intermediate states

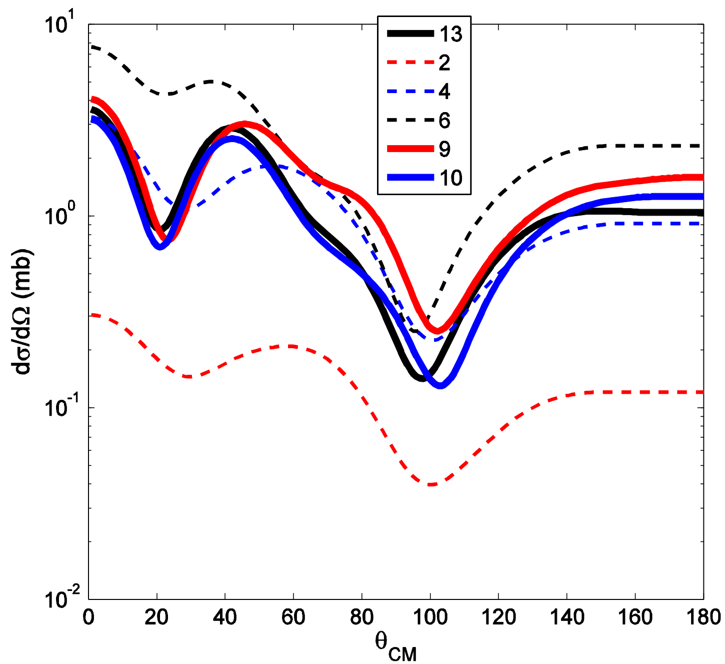

Success of second order DWBA in the calculation of absolute two-neutron transfer cross sections

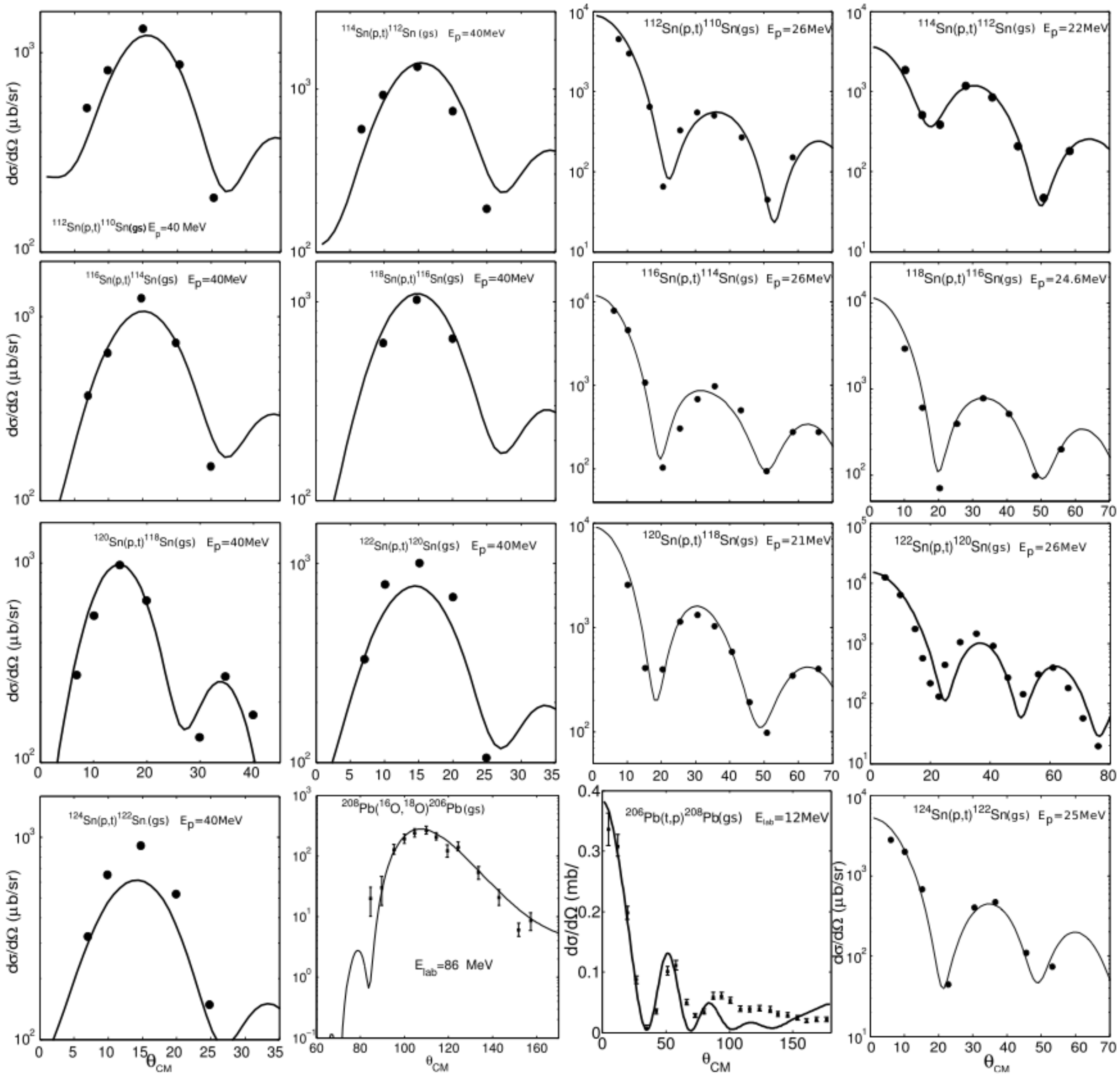

G. Potel et al., arXiV 1304.2569

Continuum particle-vibration coupling method

K. Mizuyama, G. Colo', E.V. ***Phys. Rev. C 86, 034318 (2012)***

Self-consistent Skyrme Hartree-Fock

- Description of the single particle motion in a nucleus.

Self-consistent Skyrme continuum RPA

- Description of the vibration of the nucleus.

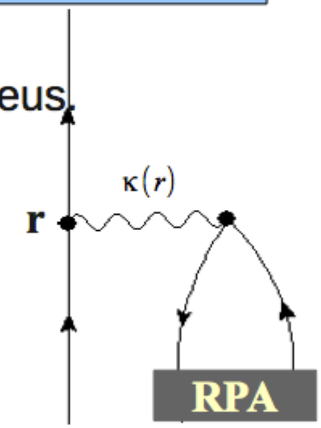

PVC Hamiltonian

$$\hat{H}_{PVC} = \int d\boldsymbol{r}\,\delta\hat{\rho}(\boldsymbol{r})\kappa(\boldsymbol{r})\sum_{\sigma}\hat{\psi}^{\dagger}(\boldsymbol{r}\sigma)\hat{\psi}(\boldsymbol{r}\sigma)$$

Self-energy function

$$\Sigma(\boldsymbol{r}\sigma,\boldsymbol{r}'\sigma';\omega) = \int_{-\infty}^{\infty}\frac{d\omega'}{2\pi}\kappa(\boldsymbol{r})\underline{G(\boldsymbol{r}\sigma,\boldsymbol{r}'\sigma';\omega-\omega')}\kappa(\boldsymbol{r}')\underline{iR(\boldsymbol{r},\boldsymbol{r}';\omega')}$$

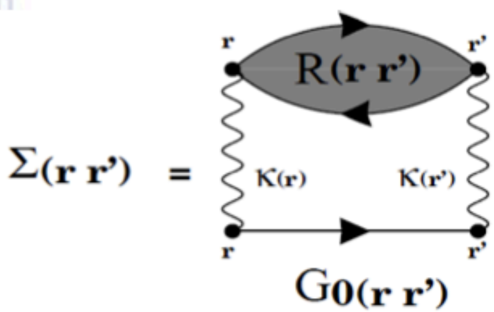

Continuum HF Green's function

Continuum RPA

$$G_{0,lj}(rr';E) = \frac{1}{W(u,v)}u_{lj}(r_<;E)v_{lj}(r_>;E)$$

Self-energy function

$$\Sigma_{lj}(rr';\omega) = \sum_{l'j',L} \frac{|\langle lj||Y_L||l'j'\rangle|^2}{2j+1}\int_{-\infty}^{\infty}\frac{d\omega'}{2\pi}\frac{\kappa(r)}{r^2}G_{0,l'j'}(rr';\omega-\omega')\frac{\kappa(r')}{r'^2}\, iR_L(rr';\omega')$$

- Numerical contour integration on the complex energy plane.

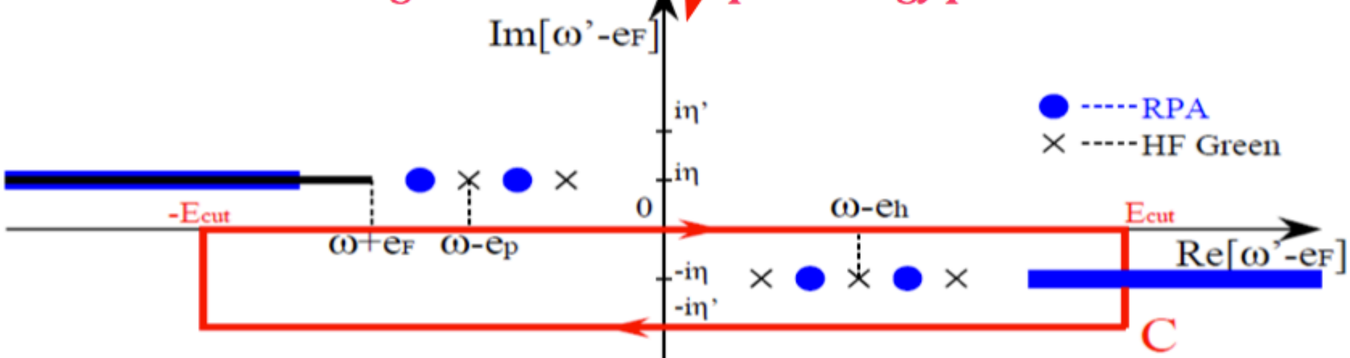

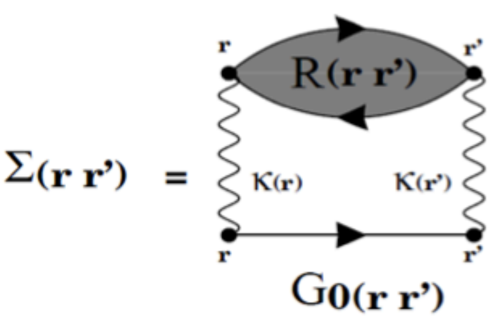

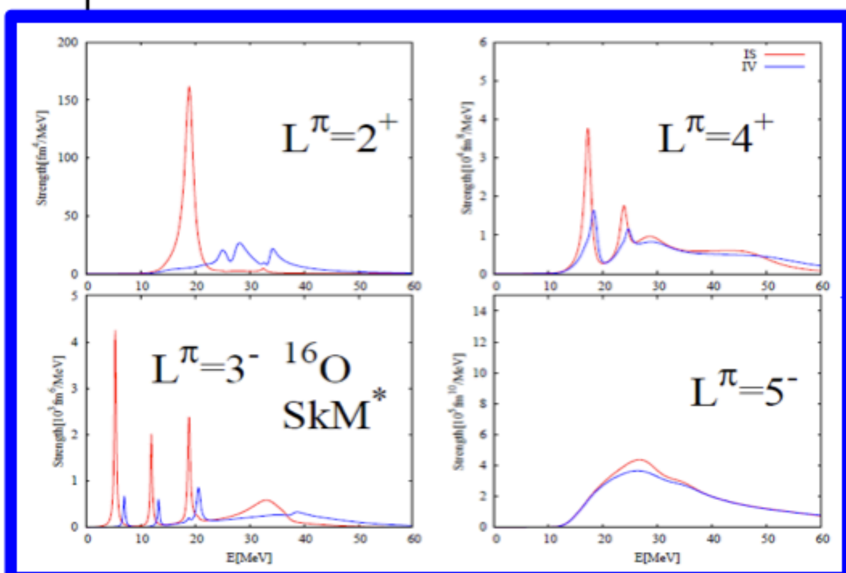

Level density and Experimental Spectroscopic factor

PHYSICAL REVIEW C 86, 034318 (2012)

HF+PVC level density

$$\bar{\rho}_{lj}(\omega) = \frac{\pm 1}{\pi} \int dr \mathrm{Im}\left(G_{lj}(rr,\omega) - G_{Free,lj}(rr,\omega)\right)$$

Cross section
→ **DWBA analysis**
(With phenomenological optical pot.)
→ **Experimental Spectroscopic factor**

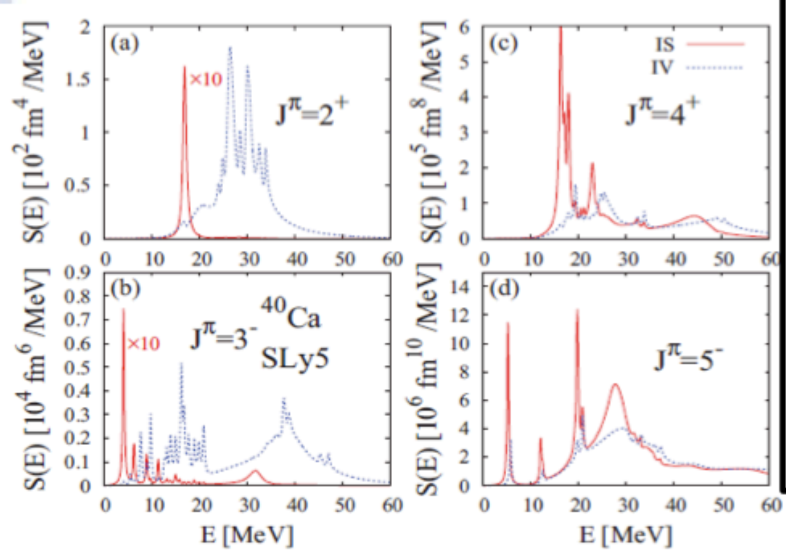

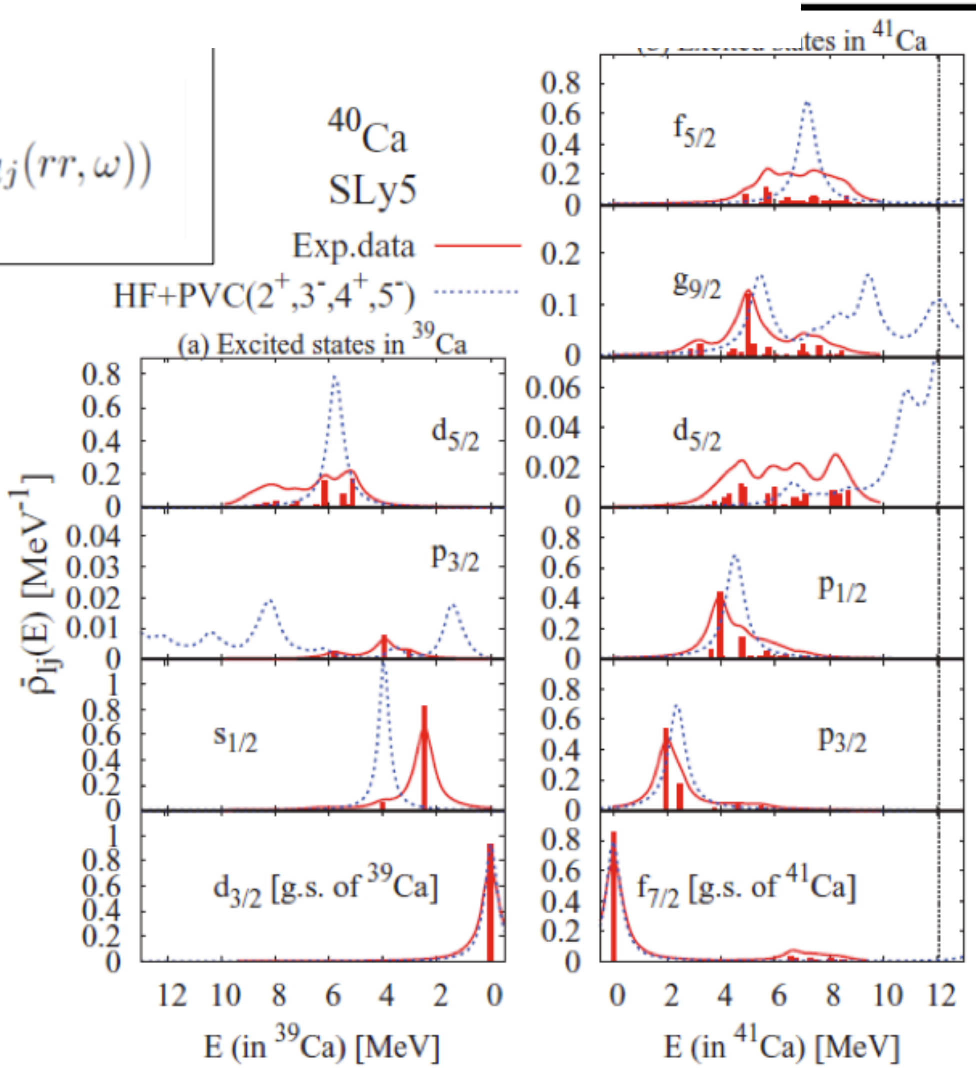

Nuclear Data Sheets 107, 225 (2006)

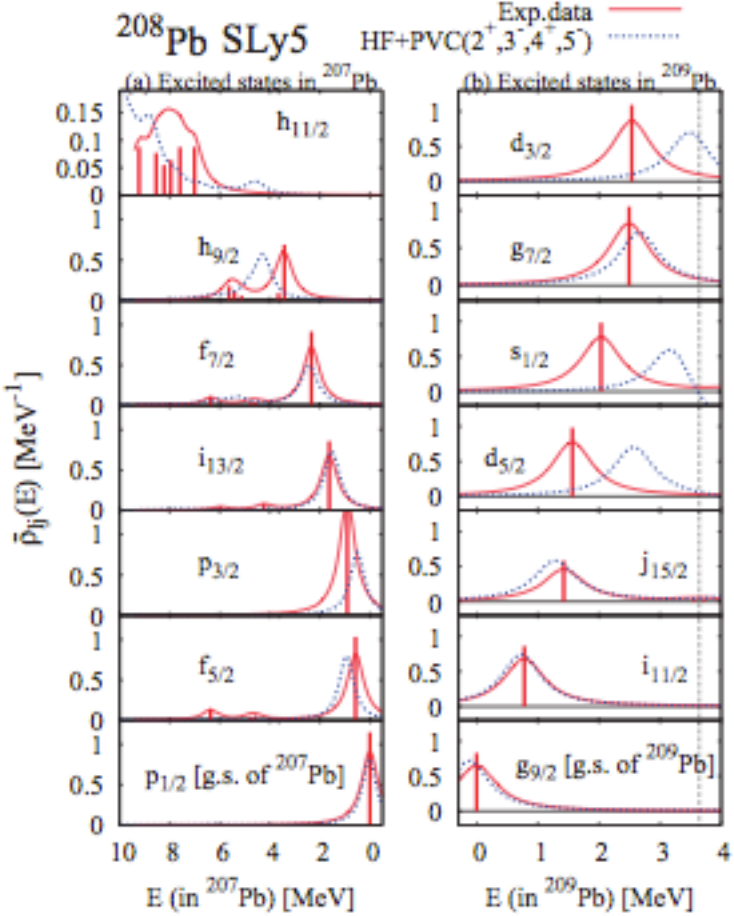

TABLE VI. The same as Table III for ^{208}Pb.

	^{208}Pb				
Holes			Particles		
J^{π}	$S_{lj}(^{207}\mathrm{Pb})$		J^{π}	$S_{lj}(^{209}\mathrm{Pb})$	
	Exp.	Theory		Exp.	Theory
$p_{1/2}$	1.07	0.82	$g_{9/2}$	0.76	0.77
$p_{3/2}$	1.50	0.84	$s_{1/2}$	0.87	0.47
$f_{5/2}$	1.07	0.84	$d_{3/2}$	0.93	0.52
$f_{7/2}$	1.02	0.84	$d_{5/2}$	0.85	0.75
$h_{9/2}$	1.06	0.86	$g_{7/2}$	0.90	0.74
$h_{11/2}$	0.39	0.39	$i_{11/2}$	0.82	0.82
$i_{13/2}$	0.90	0.87	$j_{15/2}$	0.54	0.71

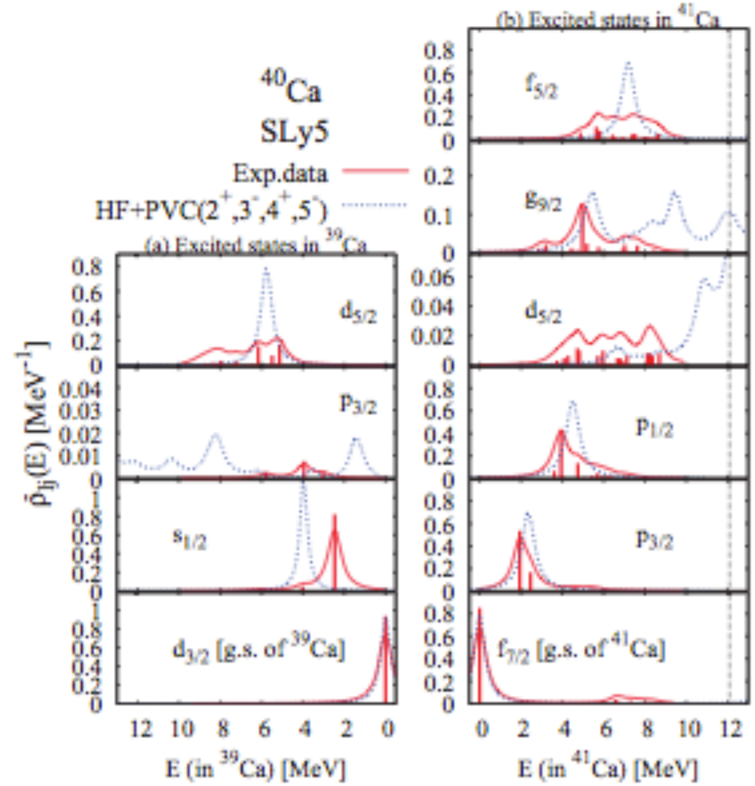

TABLE III. Experimental spectroscopic factors S_{lj} obtained from one-nucleon transfer reactions for hole and particle states in ^{39}Ca and ^{41}Ca, compared to the integral of the theoretical level density performed up to an excitation energy of 10 MeV (cf. Fig. 13).

	^{40}Ca				
Holes			Particles		
J^{π}	$S_{lj}(^{39}\mathrm{Ca})$		J^{π}	$S_{lj}(^{41}\mathrm{Ca})$	
	Exp.	Theory		Exp.	Theory
$d_{3/2}$	0.88	0.80	$f_{7/2}$	0.74	0.66
$s_{1/2}$	0.84	0.80	$p_{1/2}$	0.80	0.81
$p_{3/2}$	2.9×10^{-3}	0.05	$p_{3/2}$	0.73	0.79
$d_{5/2}$	0.73	0.75	$d_{5/2}$	0.11	0.04
			$f_{5/2}$	0.88	0.77
			$g_{9/2}$	0.28	0.36

T-matrix and continuum PVC

PHYSICAL REVIEW C 86, 041603(R) (2012)

Self-consistent microscopic description of neutron scattering by 16O based on the continuum particle-vibration coupling method

Kazuhito Mizuyama and Kazuyuki Ogata

Lippman-Schwinger equation

$$\Psi^{(+)}_{PVC}(\boldsymbol{r}\sigma,\boldsymbol{k}) = \phi_F(\boldsymbol{r}\sigma,\boldsymbol{k}) + \sum_{\sigma_1\sigma_2}\int\int d\boldsymbol{r}_1 d\boldsymbol{r}_2 G^{(+)}(\boldsymbol{r}\sigma\boldsymbol{r}_1\sigma_1;\omega)\left[v(\boldsymbol{r}_1\sigma_1)\delta(\boldsymbol{r}_1-\boldsymbol{r}_2)\delta_{\sigma_1\sigma_2} + \Sigma(\boldsymbol{r}_1\sigma_1,\boldsymbol{r}_2\sigma_2;\omega)\right]\phi_F(\boldsymbol{r}_2\sigma_2,\boldsymbol{k})$$

$$T^{PVC}_{lj}(E) = \lim_{r\to\infty}\frac{2i}{rh_l(kr)}\left[\int dr_1 G^{+}_{lj}(rr_1;E)\tilde{v}_{lj}(r_1)r_1 j_l(kr_1) + \int\int dr_1 dr_2 G^{+}_{lj}(rr_1;E)\Sigma_{lj}(r_1r_2;E)r_2 j_l(kr_2)\right],$$

$$\sigma(E) = \sum_{lj}\sigma_{lj}(E),$$

$$\sigma_{lj}(E) = \frac{2\pi}{k^2}\frac{2j+1}{2}\left[Im\ T_{lj}(E)\right]$$

$$\sigma^{el}(E) = \sum_{lj}\sigma^{el}_{lj}(E),$$

$$\sigma^{el}_{lj}(E) = \frac{\pi}{k^2}\frac{2j+1}{2}|T_{lj}(E)|^2$$

$$G(rr') = (1-G_0\Sigma)^{-1}G_0(rr').$$

$$\Sigma_{lj}(rr';\omega) = \sum_{l'j',L}\frac{|\langle lj||Y_L||l'j'\rangle|^2}{2j+1}\int_{-\infty}^{\infty}\frac{d\omega'}{2\pi}\frac{\kappa(r)}{r^2}G_{0,l'j'}(rr';\omega-\omega')\frac{\kappa(r')}{r'^2}iR_L(rr';\omega')$$

K. Mizuyama, K. Ogata PRC 86 041603(2012)

Role of transfer?

No free parameter !

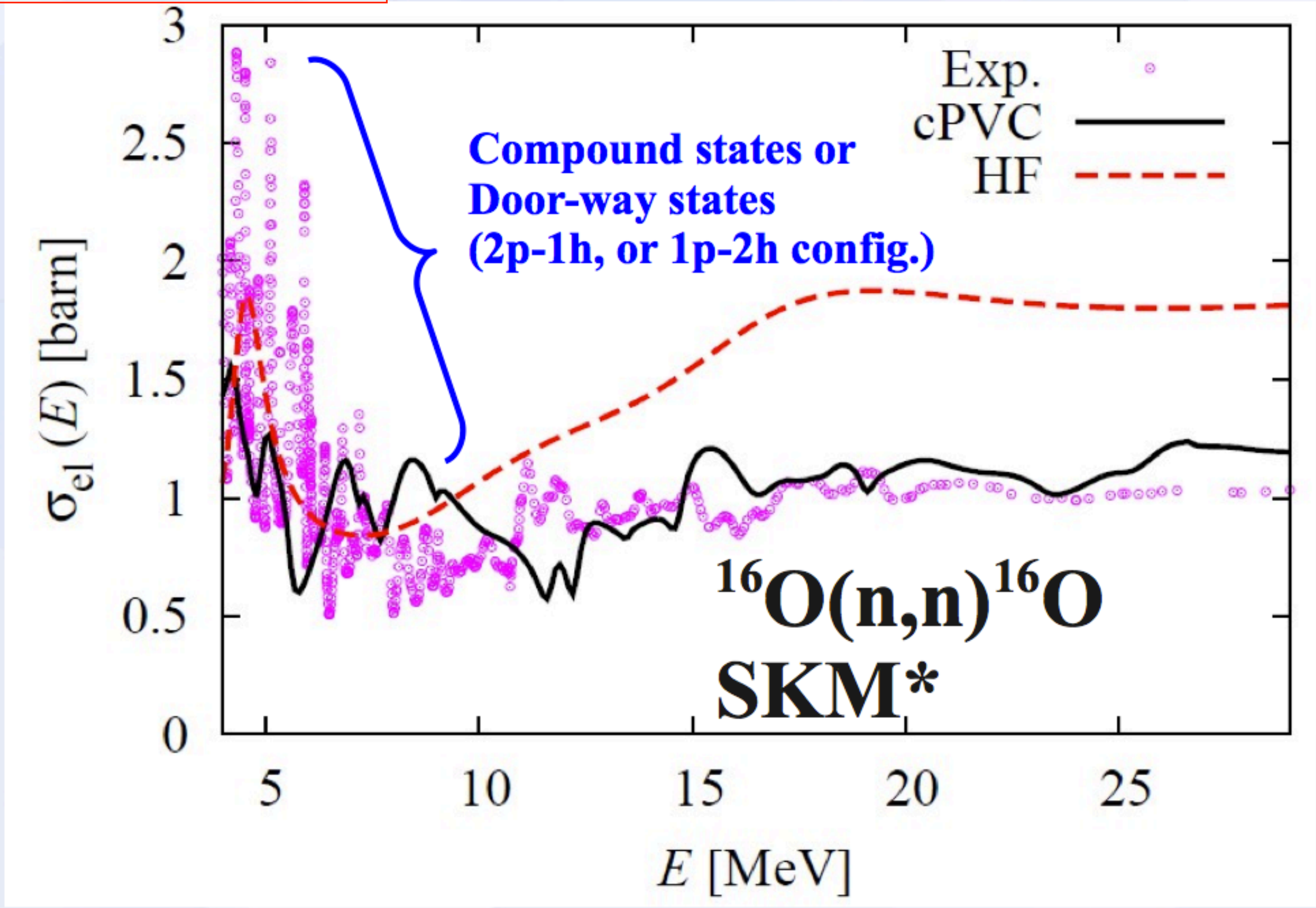

Reaction Cross section

$$\sigma_R(E) = \sigma_{\mathrm{tot}}(E) - \sigma_{\mathrm{el}}(E).$$

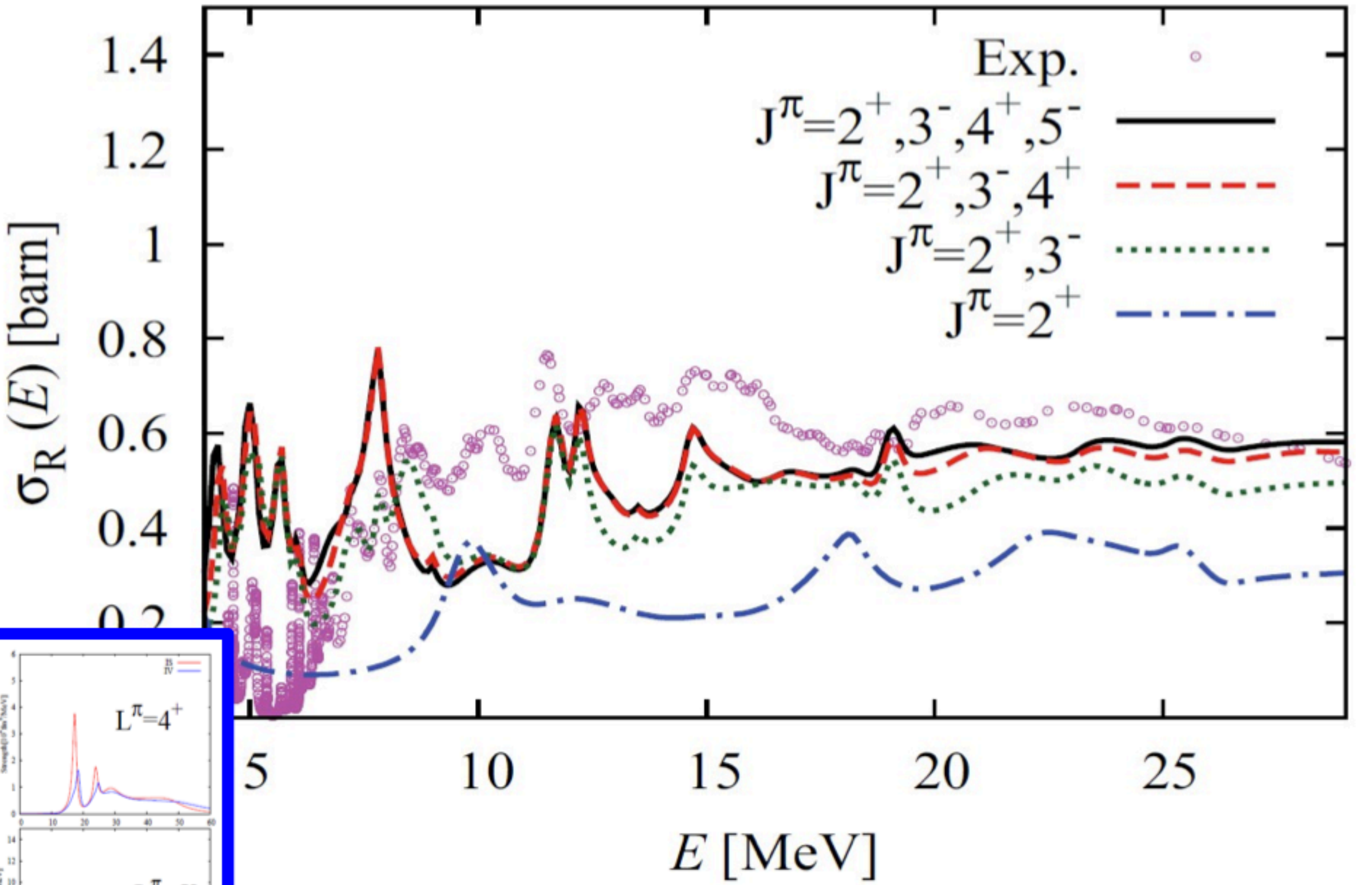

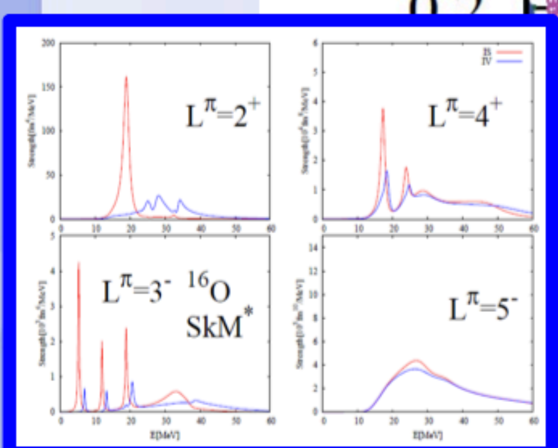

Representative calculations of optical potentials

J.P.Jeukenne, A. Lejeune, C. Mahaux PRC 10, 80 (1977)
Energy dependent optical potential in infinite matter
+ local density approximation

N. Vinh Mau, A. Bouyssy, Nucl. Phys. A371, 173 (1976)
V. Bernard, N. Van Giai, Nucl. Phys. A327, 397 (1979)
Self energy calculated in RPA with effective interactions

J.M. Mueller et al., PRC 83, 064605 (2011)
Optical potentials obtained from dispersion relations fitting elastic scattering data

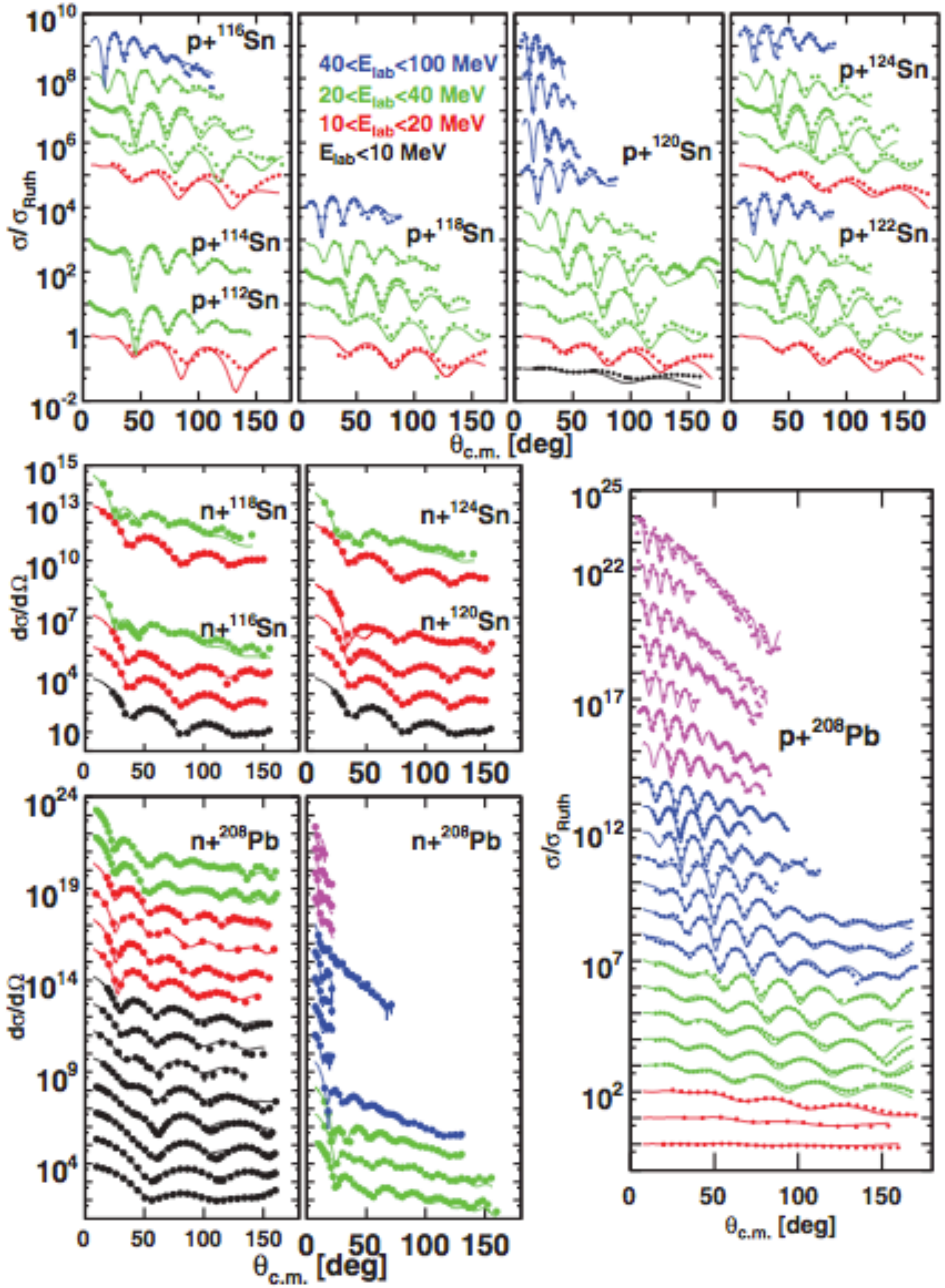

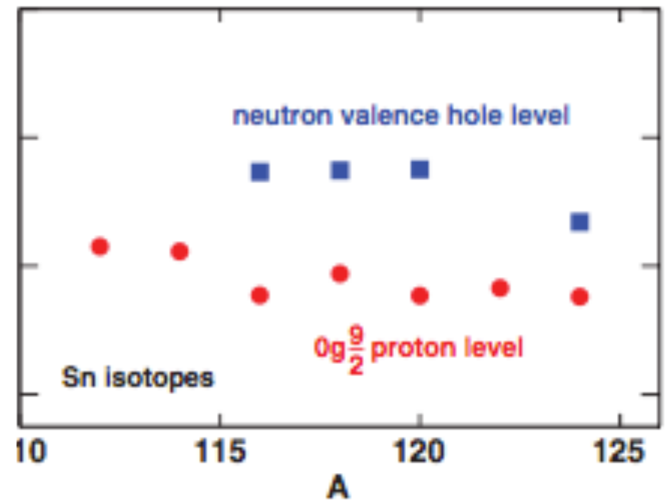

J.M. Mueller et al.,
PRC 83, 064605 (2011)

S.J. Waldecker, C. Barbieri, W.H. Dickhoff,
PRC 84,034316 (2011)
Self-energy calculated in FRPA with G-matrix from AV18

$$
\begin{aligned}
\Sigma^{\ell j}_{n_a,n_b}(E) = & \sum_r \frac{(E-\varepsilon_r)}{(E-\varepsilon_r)^2+[\Gamma(\varepsilon_r)]^2} m^r_{n_a} m^r_{n_b} \\
& + i \Bigg[\theta(E_F - E) \sum_h \frac{\Gamma(\varepsilon_h)}{(E-\varepsilon_h)^2+\Gamma(\varepsilon_h)^2} m^h_{n_a} m^h_{n_b} \\
& - \theta(E - E_F) \sum_p \frac{\Gamma(\varepsilon_p)}{(E-\varepsilon_p)^2+[\Gamma(\varepsilon_p)]^2} m^p_{n_a} m^p_{n_b} \Bigg],
\end{aligned}
$$

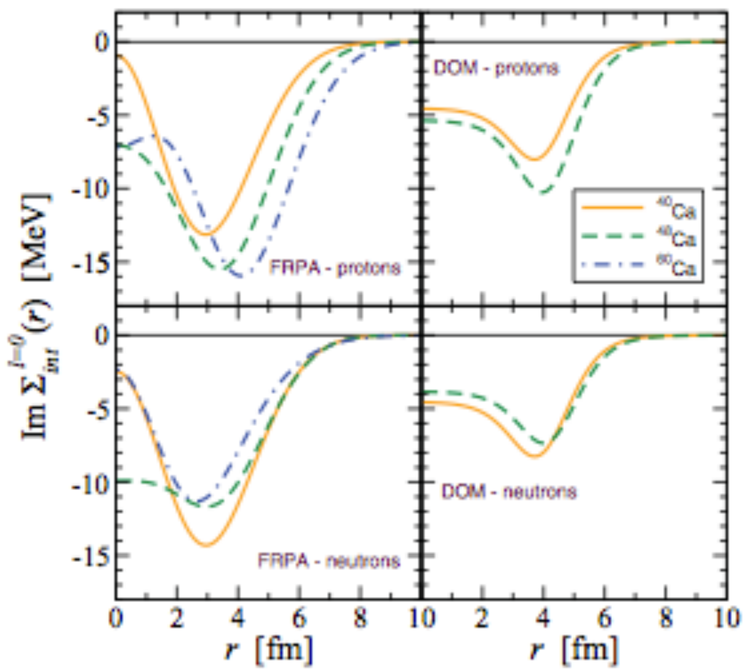

G.P.A. Nobre et al., PRC 84, 064609 (2011)
Calculation of reaction cross section with explicit inclusion of inelastic and transfer channels using transition potentials computed in QRPA

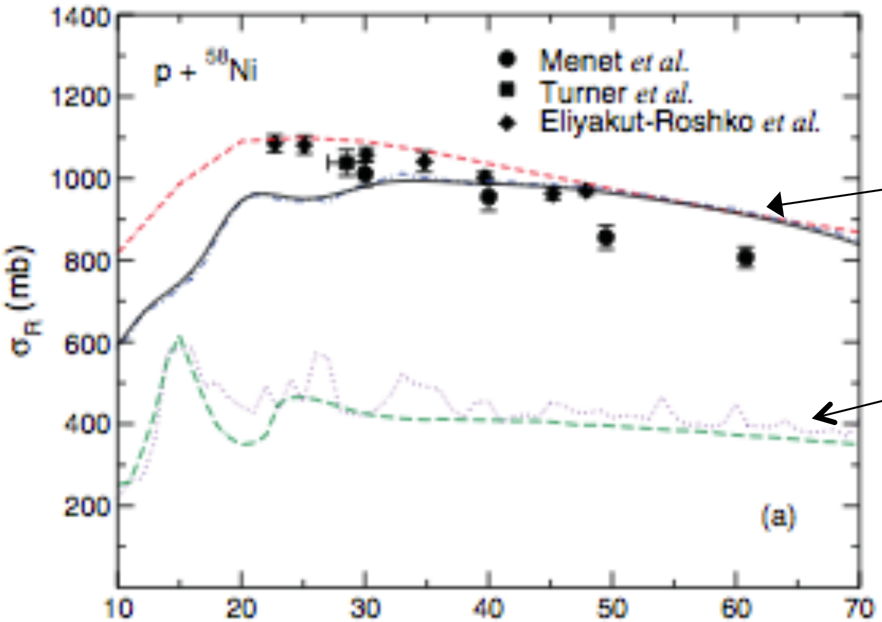

Inelastic+ pickup

Inelastic

PAIRING GAP IN FINITE NUCLEI

PAIRING GAP IN NEUTRON MATTER

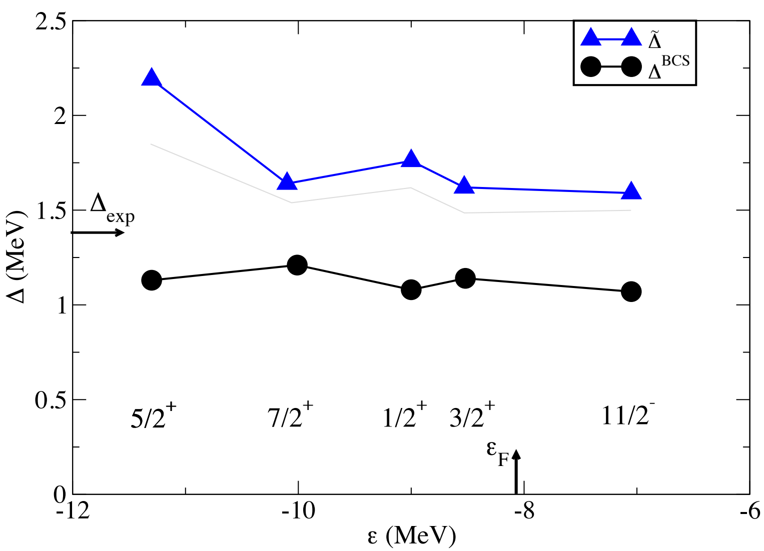

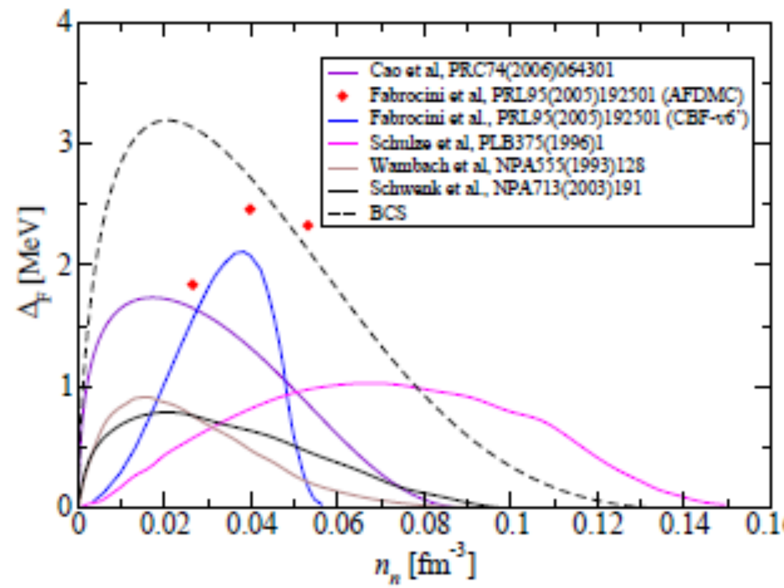

Medium effects increase the gap

Medium effects decrease the gap

The inner crust: coexistence of a Coulomb lattice of finite nuclei with a sea of free neutrons

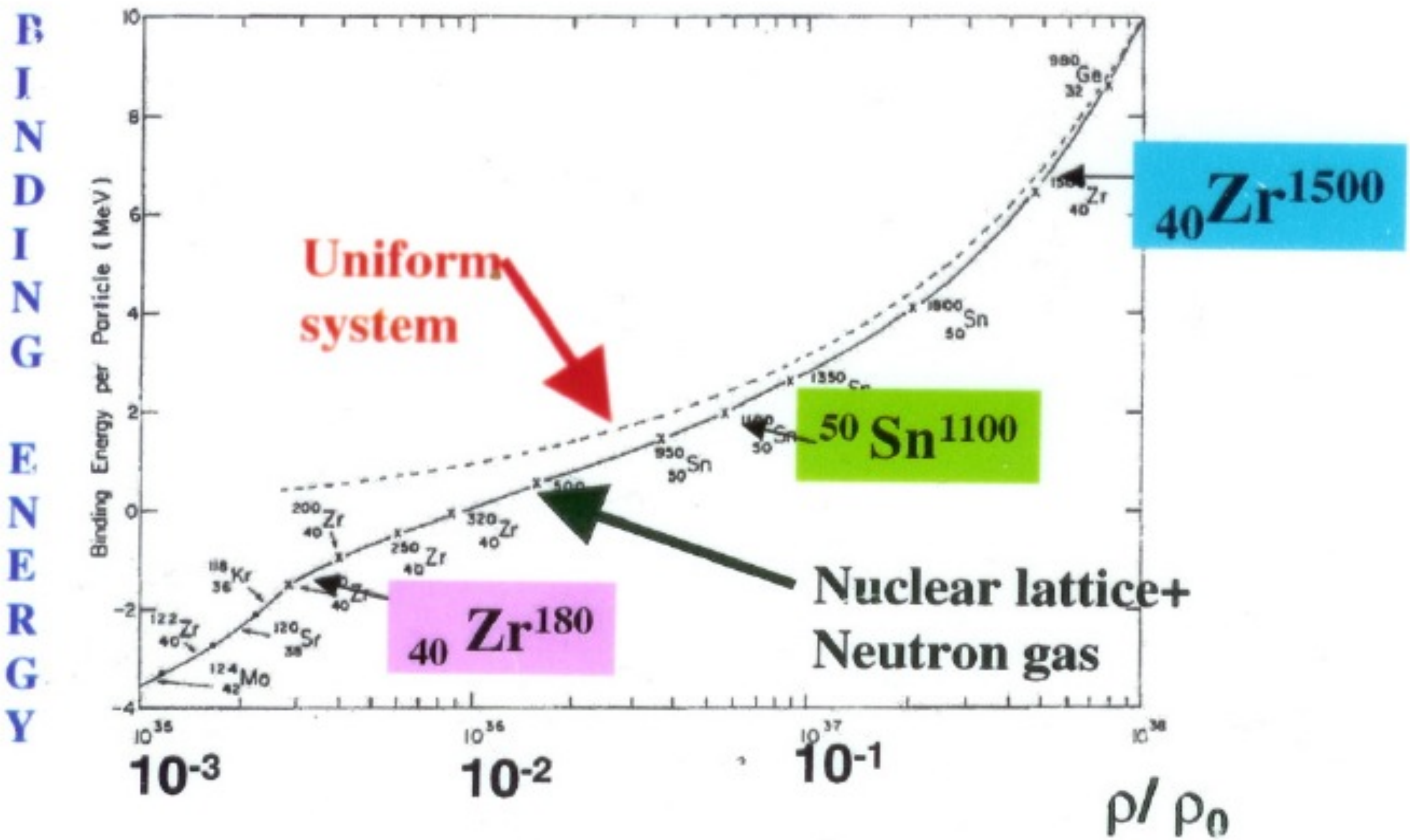

J. Negele, D. Vautherin
Nucl. Phys. A207 (1974) 298

M. Baldo et al
Nucl. Phys. A750 (2005) 409

Lattice of heavy nuclei surrounded by a sea of superfluid neutrons.

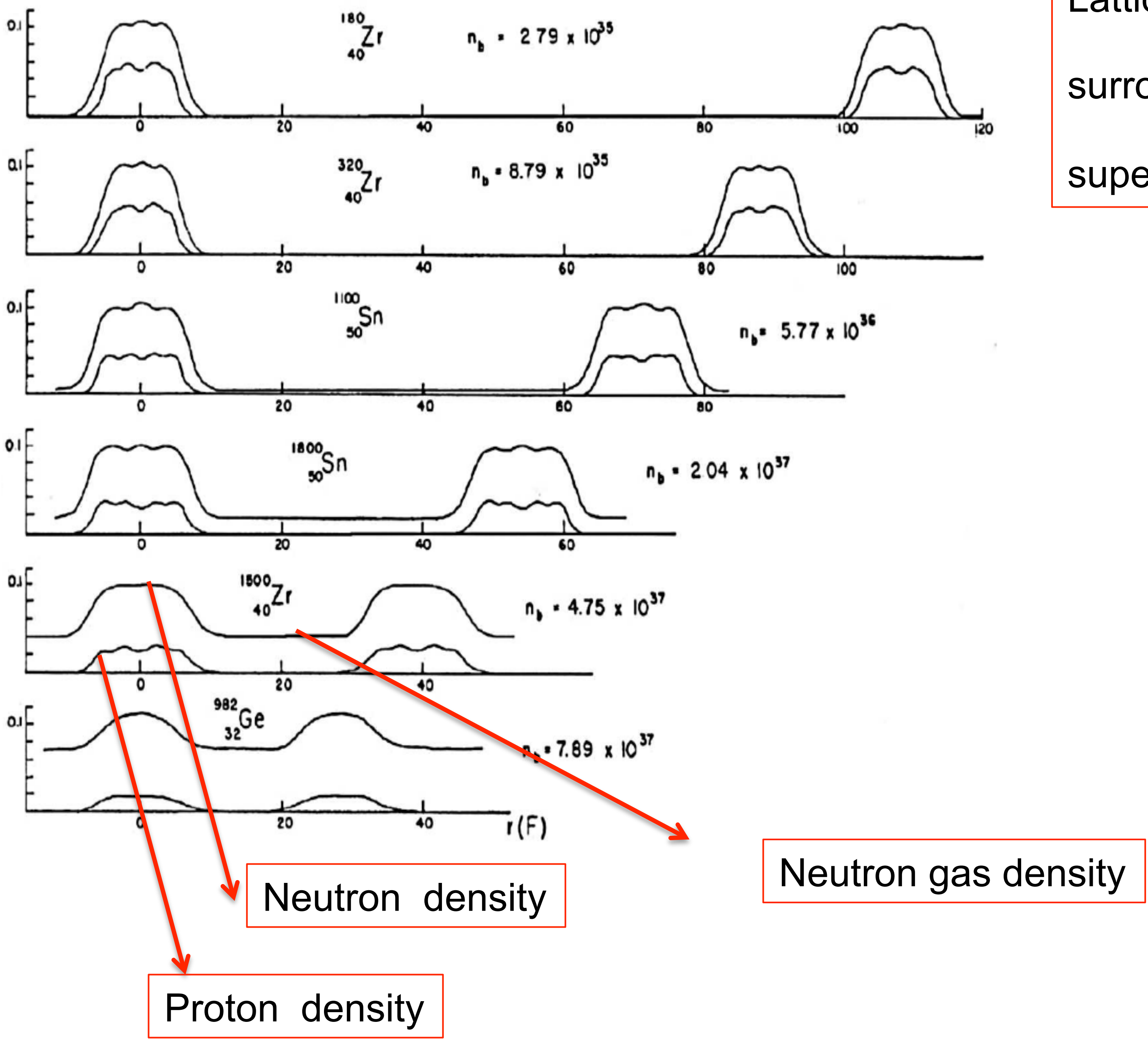

Going beyond mean field within the Wigner-Seitz cell: including the effects of polarization (exchange of vibrations) and of finite nuclei at the same time

Spin modes

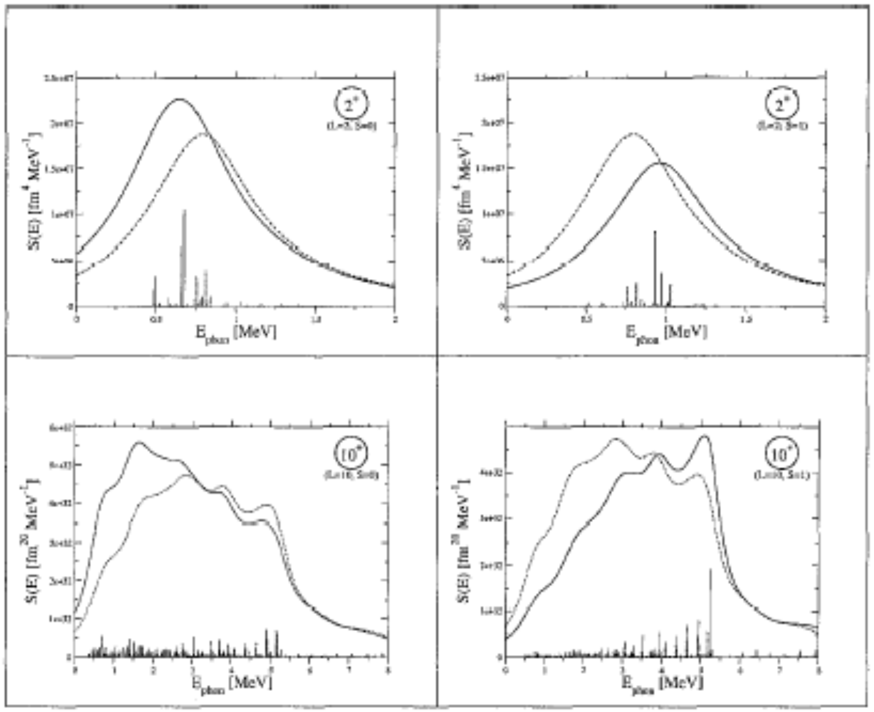

RPA response

Induced pairing interaction

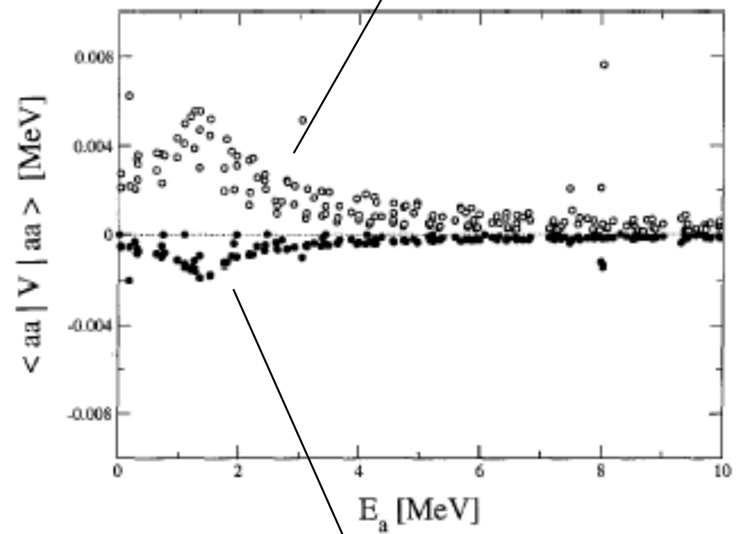

Density modes

G. Gori, F. Ramponi, F. Barranco,R.A. Broglia,
G. Colo, D. Sarchi,E. Vigezzi, NPA731(2004)401

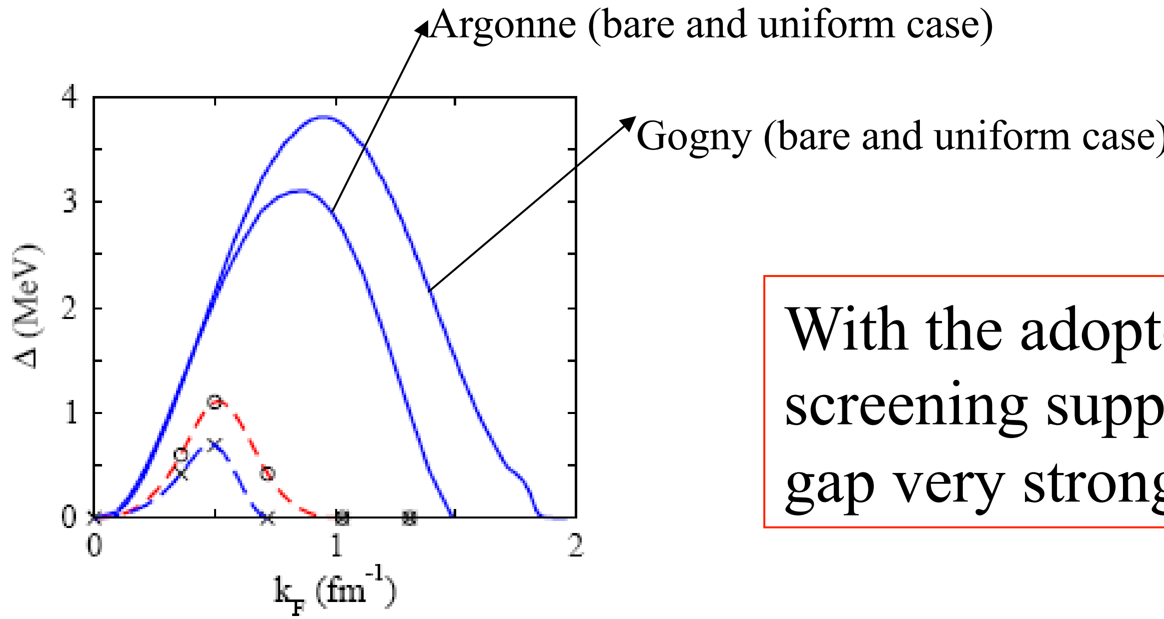

With the adopted interaction, screening suppresses the pairing gap very strongly for $k_F > 0.7\ fm^{-1}$

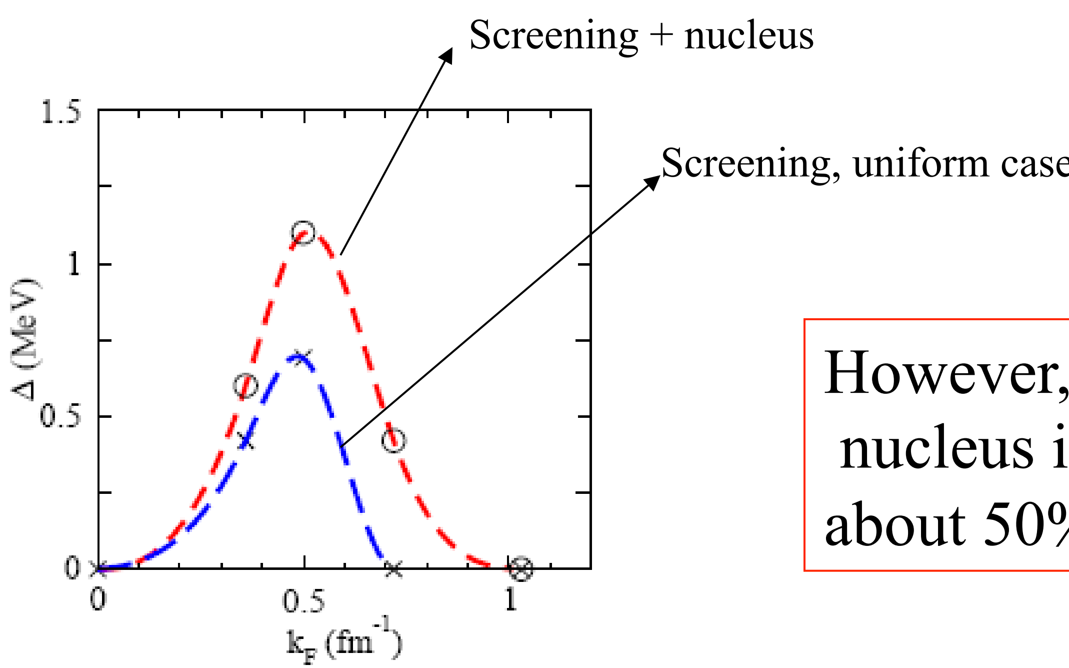

However, the presence of the nucleus increases the gap by about 50%

A challenge: calculation of the self-energy in the Wigner-Seitz cell.
Until now, only preliminary calculations of the pairing induced interaction exist

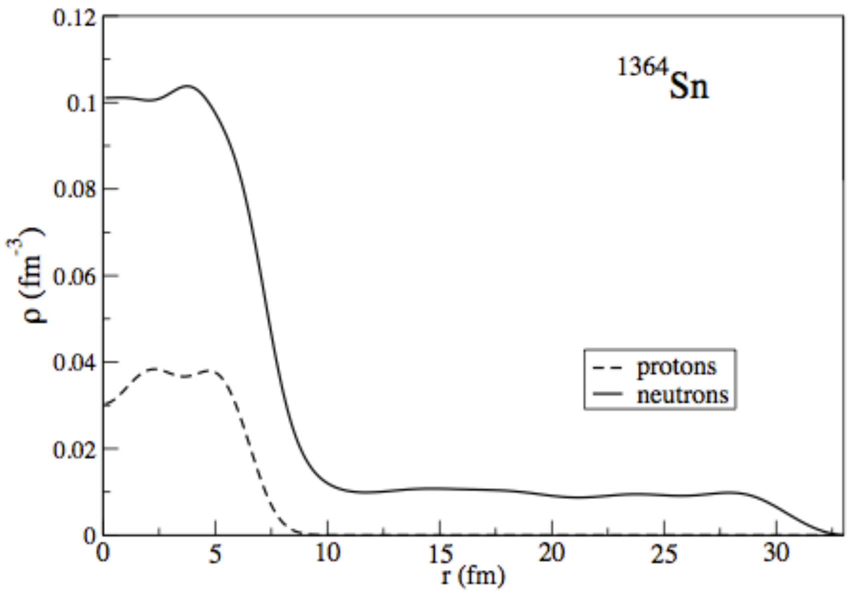

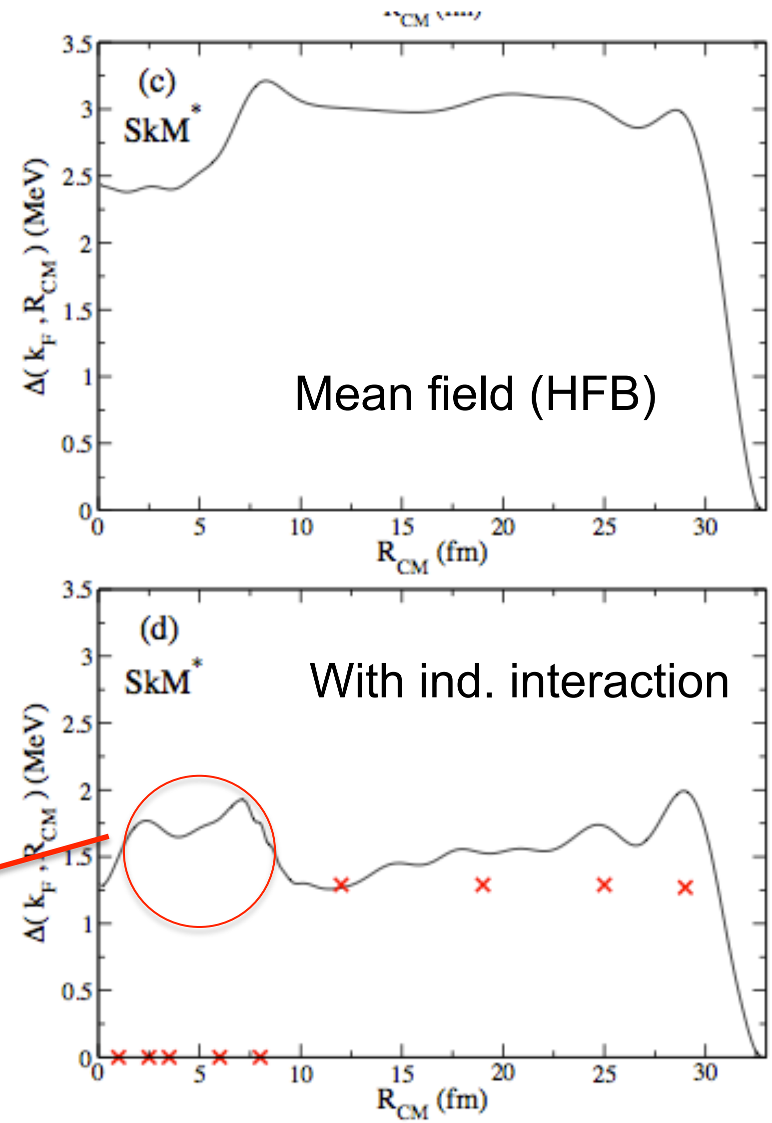

The gap is quenched in the interior of the nucleus, but much less than in neutron matter at the same density

S. Baroni et al., arXiv:0805.3962